



**FAKULTA
STROJNÍ
ČVUT V PRAZE**

Ústav mechaniky, biomechaniky a mechatroniky

**Optimalizace využití energie hybridního
monopostu Formule Student**

**Optimization of energy usage of Formula
Student hybrid monopost**

**DIPLOMOVÁ PRÁCE
2022**

Bc. Tomáš Adamec

Studijní program: Aplikované vědy ve strojním inženýrství

Specializace: Mechatronika

Vedoucí práce: Prof. Ing. Zbyněk Šika, Ph.D.

Konzultant práce: Ing. Petr Denk, Ph.D.

I. OSOBNÍ A STUDIJNÍ ÚDAJE

Příjmení: **Adamec** Jméno: **Tomáš** Osobní číslo: **466507**
Fakulta/ústav: **Fakulta strojní**
Zadávací katedra/ústav: **Ústav mechaniky, biomechaniky a mechatroniky**
Studijní program: **Aplikované vědy ve strojním inženýrství**
Specializace: **Mechatronika**

II. ÚDAJE K DIPLOMOVÉ PRÁCI

Název diplomové práce:

Optimalizace využití energie hybridního monopostu Formule Student

Název diplomové práce anglicky:

Optimization of energy usage of Formula Student hybrid monopost

Pokyny pro vypracování:

- 1) Seznamte se s koncepty hybridních vozidel a optimalizací jejich energetické spotřeby.
- 2) Seznamte se s modely závodního okruhu a vozidla vhodnými pro simulaci.
- 3) Navrhněte a vytvořte model hybridního pohonu pro uvažovaný monopost.
- 4) Navrhněte koncept řízení hybridního pohonu.
- 5) Proveďte citlivostní analýzu celé úlohy vzhledem k parametrům ovládání hybridního pohonu.
- 6) Na spojeném modelu okruhu a vozidla s pohonem proveďte optimalizace doby jízdy při využití omezeného množství energie.

Seznam doporučené literatury:

- [1] Denk, P., Optimalizace jízdy silničního motorového vozidla, Disertační práce, České vysoké učení technické v Praze, Fakulta strojní, 2020.
[2] Novotný T., Výpočet teoretického času vozidla na závodním okruhu, Diplomová práce, České vysoké učení technické v Praze, Fakulta strojní, 2016.
[3] Boehme, T., J. et al., Solutions of Hybrid Energy-Optimal Control for Model-based Calibrations of HEV Powertrains, SAE Technical Paper 2013-01-1747, 8 04 2013.
[4] Salazar, M. et al., Optimal Control Policy Tuning and Implementation for a Hybrid Electric Race Car. IFAC-PapersOnLine, 2016. 49. 147-152.

Jméno a pracoviště vedoucí(ho) diplomové práce:

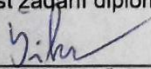
prof. Ing. Zbyněk Šika, Ph.D. odbor mechaniky a mechatroniky FS

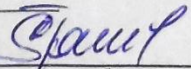
Jméno a pracoviště druhé(ho) vedoucí(ho) nebo konzultanta(ky) diplomové práce:

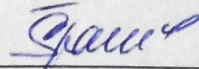
Datum zadání diplomové práce: **22.04.2022**

Termín odevzdání diplomové práce: **15.08.2022**

Platnost zadání diplomové práce:


prof. Ing. Zbyněk Šika, Ph.D.
podpis vedoucí(ho) práce



doc. Ing. Miroslav Španiel, CSc.
podpis vedoucí(ho) ústavu/katedry


doc. Ing. Miroslav Španiel, CSc.
podpis děkana(ky)

III. PŘEVZETÍ ZADÁNÍ

Diplomant bere na vědomí, že je povinen vypracovat diplomovou práci samostatně, bez cizí pomoci, s výjimkou poskytnutých konzultací. Seznam použité literatury, jiných pramenů a jmen konzultantů je třeba uvést v diplomové práci.

1.6.2022
Datum převzetí zadání


Podpis studenta

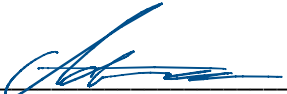
PREHLÁSENIE

Prehlasujem, že som diplomovú prácu s názvom

Optimalizace využití energie hybridního monopostu Formule Student

vypracoval samostatne, iba s prispením vedúceho práce a konzultanta a použil som k tomu iba pramene v práci uvedené. Prehlasujem, že nemám námietky proti využitiu výsledkov tejto práce fakultou ani proti jej zverejňovaniu so súhlasom vedúceho práce.

V Praxe dňa 15.8.2022



Bc. Tomáš Adamec

ABSTRAKT

Práca sa zaoberá skúmaním možností na úsporu a optimálne využitie energie s cieľom minimalizácie času na prejazd Formula Student vozidla vopred definovanou traťou.

V rámci práce bol navrhnutý riadiaci algoritmus hybridného pohonu vozidla s variabilnými parametrami, ktoré určujú intenzitu generovania a úspory energie. Dopad tohto algoritmu bol vyhodnocovaný pomocou nástroja na výpočet teoretického času na prejazd vozidla definovanou traťou na základe maximálnych adhézných možností vozidla a špecifikovaného modelu pohonného ústrojenstva rozšíreného o hybridný pohon. Vhodné parameter riadiaceho algoritmu boli nájdené použitím matematickej optimalizácie.

Záver práce obsahuje zhodnotenie prínosu navrhnutého algoritmu na vybranej testovacej trati a stručný popis krokov odporúčaných pred implementáciou algoritmu do reálneho vozidla.

Klíčové slová

Hybrid, optimalizace, závodní vozidlo, Formula Student, Matlab, Simulink

ABSTRACT

This thesis explores opportunities for saving and optimal usage of energy with the goal of minimizing lap time of a Formula Student vehicle on a pre-defined track.

Within the scope of this work a concept of a control algorithm for the hybrid powertrain of the vehicle was designed. The algorithm has variable parameters, which determine the intensity of energy generation and saving. The impact of this algorithm was evaluated using a tool designed for estimation of lap time on a given racing course based on a vehicle performance envelope defined by maximal adhesion capabilities and a model of longitudinal dynamics extended by a model of the hybrid powertrain. Appropriate values of the control algorithm parameters were determined by mathematical optimization of the problem.

The conclusion of the thesis sums up the benefits of the proposed algorithm on a given test track with a brief proposal of steps needed for an implementation of the algorithm in the real vehicle.

Key words

Hybrid, optimization, race car, Formula Student, Matlab, Simulink

POĎAKOVANIE

Veľká vďaka patrí vedúcemu mojej diplomovej práce prof. Ing. Zbyňkovi Šikovi, Ph.D. a konzultantovi práce Ing. Petrovi Denkovi, Ph.D. za množstvo cenných rád, postrehov a myšlienok, ktorými mi pomohli pri návrhu a realizácii tejto práce.

Rád by som týmto poďakoval aj celej mojej rodine a blízkym za ich trpezlivosť a podporu ako pri vypracovaní tejto práce, tak aj počas celého štúdia. Vďačím im za možnosť študovať na vysokej škole a nasledovať svoje sny.

V neposlednej rade patrí veľká vďaka tímu CTU CarTech vrátane jeho bývalých aj súčasných členov, ktorí dnes tvoria moju druhú rodinu s ktorou sme za roky pôsobenia v tíme prekonalí nespočet problémov, zažili kopu zážitkov a dosiahli mnoho úspechov. Verím, že okrem tejto práce, budem zo skúseností a vedomostí nadobudnutých v tíme čerpať aj po zvyšok môjho života.

Vďaka patrí aj všetkým partnerom tímu CTU CarTech, ku ktorým neoddeliteľne patrí aj samotné České vysoké učenie technické v Prahe, za umožnenie realizovať množstvo zaujímavých projektov a získať tak praktické skúsenosti a vedomosti aj nad rámec bežného štúdia.

Ďakujem aj kolegom z Encore Technologies za ich trpezlivosť, pochopenie a podporu pri celom štúdiu a obzvlášť v období vypracovania tejto práce.

TABLE OF FIGURES

Figure 1 - Skidpad track layout [1] _____	5
Figure 2 - Formula Student East 2021 Endurance track _____	6
Figure 3 - schematic diagram of series hybrid vehicle [5] _____	8
Figure 4 - schematic diagram of parallel hybrid vehicle [5] _____	8
Figure 5 - schematic diagram of series/parallel hybrid vehicle [5] _____	9
Figure 6 - diagram of different topology types of a MHEV [8] _____	11
Figure 7 - FS.14 on Acceleration event at FS Czech 2022 _____	13
Figure 8 - FS.14 side view _____	14
Figure 9 - FS.14 top view _____	14
Figure 10 - g-g measurements on a Grand Prix car [17] _____	18
Figure 11 - lateral and longitudinal acceleration versus speed and the progression around the performance envelope [18] _____	19
Figure 12 - illustration of the cornering phases on a g-g diagram _____	20
Figure 13 - lap time sensitivities of FS.13 as simulated in OptimumLap _____	22
Figure 14 - track analysis [20] _____	27
Figure 15 - Data filtering - step 1 [20] _____	28
Figure 16 - Data filtering - step 2 [20] _____	28
Figure 17 - Single-track model [20] _____	29
Figure 18 - Slowly increasing maneuver [20] _____	30
Figure 19 - corrected speed estimate - braking phase [20] _____	32
Figure 20 - corrected speed estimate - accelerating and braking [20] _____	32
Figure 21 - boundary velocity profile [20] _____	33
Figure 22 - simulation model - Stage II [20] _____	33
Figure 23 - schematic powertrain Simulink model [20] _____	34
Figure 24 - torque and power characteristic of a modified Yamaha R6 engine used on FS.14 [21] _____	34
Figure 25 - schematic powertrain model [20] _____	36
Figure 26 - BSFC map [20] _____	37
Figure 27 - longitudinal weight transfer during acceleration [17] _____	40
Figure 28 - acceleration and speed data from Acceleration event on FS.14 without hybrid power (x axis is time) _____	41
Figure 29 - TTC tire data as analyzed in OptimumTire _____	42

Figure 30 - Simulink simulation of maximal long. acceleration depending on changing speed _____	43
Figure 31 - simulation of maximal longitudinal acceleration with aerodynamic forces _____	44
Figure 32 - illustration of the rear axle limitation _____	45
Figure 33 - realization of grip limitation of the rear axle in Matlab Simulink _____	46
Figure 34 - schematic model of the powertrain _____	46
Figure 35 - Torque curve of the used electric motor [23] _____	48
Figure 36 - Efficiency curve of the used electric motor [23] _____	48
Figure 37 - battery cell discharge voltage profiles [24] _____	49
Figure 38 – illustration of filtering out the ICEs braking torque _____	52
Figure 39 – illustration of detecting the full throttle event _____	52
Figure 40 - implementation of maximal available driving torque validation _____	53
Figure 41 - v_off energy saving illustration _____	53
Figure 42 - implementation of v_off energy saving _____	54
Figure 43 – implementation of driving torque demand in Simulink _____	54
Figure 44 - illustration of a regenerative braking regulator attached to the hydraulic brake piston [25] _____	55
Figure 45 - illustration of energy generation during braking _____	58
Figure 46 – illustration of an implementation of proportional recuperation _____	58
Figure 47 - illustration of energy generation during acceleration by the ICE _____	59
Figure 48 – illustration of the implementation of acceleration recuperation _____	59
Figure 49 - illustration of energy generation during coasting _____	60
Figure 50 – illustration of implementation of coasting recuperation _____	61
Figure 51 – implementation of maximal available braking torque validation _____	61
Figure 52 – implementation of braking torque demand in Simulink _____	62
Figure 53 – implementation of SOC validation in Simulink _____	63
Figure 54 – implementation of overcurrent protection in Simulink _____	64
Figure 55 - slip ratio on a driven axle with and without traction control [27] _____	65
Figure 56 – cornering with and without torque vectoring. [28] _____	66
Figure 57 - torque vectoring (b.) improves traction and cornering by distributing torque more effectively [28] _____	67
Figure 58 - the full implementation of the electric torque control algorithm _____	68
Figure 59 - energy usage on Endurance without energy saving and recuperation _____	69
Figure 60 - optimization of first half of the Endurance using GA _____	71
Figure 61 - energy usage on Endurance after optimization of the first half _____	72
Figure 62 - optimization of the full Endurance using GA _____	73

Figure 63 - energy usage on second half of Endurance after optimization over the whole distance using GA	74
Figure 64 - optimization of the full Endurance using fminsearch	75
Figure 65 - energy usage on second half of Endurance after optimization over the whole distance using fminsearch	76
Figure 66 - results of sensitivity analysis	77
Figure 67 - Pareto front resulting from the multi-objective optimization	78

LIST OF TABLES

Table 1 - scoring of static disciplines [1] _____ 3

Table 2 - scoring of dynamic disciplines [1] _____ 4

Table 3 - strength categorization of hybrid vehicles [6] _____ 9

Table 4 - topology categorization of hybrid vehicles [7] _____ 10

Table 5 - main parameters of FS.14 _____ 14

Table 6 - main parameters of FS.14 powertrain _____ 15

Table 7 - hybrid energy storage parameters _____ 16

Table 8 - overview of times per discipline before optimization _____ 69

Table 9 - overview of optimization parameters _____ 70

Table 10 – resulting parameters after initial test of the optimization _____ 71

Table 11 - resulting parameters after full Endurance optimization using GA _____ 73

Table 12 - resulting parameters after full Endurance optimization using fminsearch
_____ 75

Table 13 - overview of times per discipline after optimization _____ 79

APPENDICES

Appendix 1: 1 CD data carrier. The CD contains the modified lap time simulation, scripts used for the analysis of friction characteristics of the vehicle, scripts used for the optimization and sample vehicle data.

CONTENTS

Prehlásenie	iii
Abstrakt	iv
Abstract	v
PodĎakovanie	vi
Table of figures	vii
List of tables	x
Appendices	xi
1. Introduction	1
2. Formula Student	3
2.1. Static disciplines	3
2.2. Dynamic disciplines	4
2.2.1. Acceleration	4
2.2.2. Skidpad	5
2.2.3. Autocross	6
2.2.4. Endurance and Efficiency	6
3. Hybrid electric vehicles	7
3.1. Main hybrid categorization	7
3.2. Strength categorization	9
3.3. Topology categorization	10
3.4. Hybrid vehicle energy optimization	11
4. CTU CarTech FS.14 concept	13
4.1. Overall FS.14 concept	14
4.2. FS.14 powertrain	15
4.3. Hybrid energy storage	16
5. The fundamentals of racing	17
5.1. The g-g and g-g-v diagram	17

5.2. Phases of cornering _____	19
6. Lap Time simulations _____	21
6.1. The current Lap Time simulations used in CTU CarTech _____	22
6.2. Steady state method _____	23
6.3. Quasi-static and quasi-transient methods _____	24
6.4. Transient method _____	24
6.5. Choice of a suitable Lap Time simulation _____	24
6.6. Choice of a simulation _____	25
7. Laptime tool description _____	26
7.1. Stage I – Initial velocity profile _____	26
7.1.1. Track analysis _____	26
7.1.2. Vehicle performance envelope _____	28
7.1.3. Initial velocity profile _____	31
7.2. Stage II – Simulation model _____	33
7.2.1. Powertrain model _____	34
7.2.2. Longitudinal dynamics _____	35
7.2.3. Fuel consumption _____	37
8. Laptime tool adjustment _____	38
8.1. Tire model _____	38
8.1.1. Lateral tire dynamics _____	38
8.1.2. Longitudinal tire dynamics _____	38
8.2. Longitudinal dynamics _____	44
8.3. The electric powertrain model _____	47
8.4. Energy consumption _____	48
9. Control algorithms _____	50
9.1. Initial drive torque demand _____	51
9.2. Recuperation control (brake torque demand) _____	55
9.2.1. The brake pedal mechanism _____	55
9.2.2. The hybrid powertrain concept _____	56

9.2.3. The brake balance and recuperation gain	56
9.3. Overcharging and overdrawing the battery (SOC validation)	62
9.4. Overcurrent protection	63
9.5. Traction control	65
9.6. Torque vectoring	66
9.7. Summary	67
10. Optimization	69
10.1. Genetic algorithms	70
10.2. Simplex method	75
10.3. Sensitivity analysis	76
10.4. Multi-objective optimization	77
10.5. Results	79
11. Conclusion	80
12. References	82

1. INTRODUCTION

The objective of this thesis is to use simulation and optimization tools to improve the energy usage of a hybrid powertrain of an already designed and manufactured race car strictly regulated by Formula Student rules. The result of this work should serve as an examination of different energy saving and recuperation strategies. These findings, together with other observations regarding the design of the race car and the examination of different advanced control algorithms for the hybrid system should serve as a basis for the design of the next generation vehicle for the next racing season.

Goals of this work can be summarized in the following 6 points:

1. Research different concepts of hybrid vehicles and their approach to optimization of energy consumption
2. Research track and vehicle models suitable for the simulation
3. Design and create a model of a hybrid powertrain for the monopost
4. Propose a concept of a control algorithm for the hybrid powertrain
5. Perform a sensitivity analysis of the whole problem with respect to the parameters of the control algorithm
6. On the model of the track and the vehicle, perform an optimization of lap time with limited energy for the hybrid powertrain

For the reader to easily understand the context of this thesis, chapters 2 and 4 serve as an introduction to the Formula Student competition and as a brief description of the vehicle concept which is the subject of this thesis.

Chapters 3, 5 and 6 provide a theoretical basis for topics and concepts on which the thesis is built and which will be used and referenced throughout this work. Additional theoretical paragraphs concerning for example vehicle dynamics or the optimization methods will be placed in relevant chapters to provide further context for the topic at hand.

Chapters 7 provides a detailed description of a simulation tool I used for this work and the chapter 8 then describes the necessary changes I did to this tool to fit this application.

The main body of this work, the chapters 9 and 10, describes the proposed energy saving and recuperation strategies together with a brief examination of advanced control strategies, which can be used for the hybrid system. In the chapter 10, the parameters of the proposed control algorithm are optimized to minimize lap time on the main dynamic discipline of the Formula Student competition.

Lastly, a commentary on an overall success of this work together with references to the goals specified in this chapter is provided in the Conclusion of this thesis.

2. FORMULA STUDENT

Formula Student is an international engineering competition in which university students must conceive, design, manufacture and compete with prototype, formula style, race cars. The competition first started in USA in year 1981. The first race in Europe was held in 1998 and since then the competition has spread most parts of the world. Currently there are more than 600 competing teams in the combustion category and more than 200 teams in the electric category. With these numbers, Formula Student is the largest engineering competition in the world. The competition consists of 8 disciplines and teams must demonstrate their skills and knowledge in engineering as well as in management, marketing and basic economics.

2.1. Static disciplines

Static disciplines are events, where professionals from the automotive industry judge the theoretical knowledge of the teams and its implementation during the production of the vehicle.

Table 1 - scoring of static disciplines [1]

Discipline	Maximum points
Engineering design	150
Cost and manufacturing	100
Business plan presentation	75

2.2. Dynamic disciplines

The performance of the vehicle is directly tested in 5 dynamic disciplines.

Table 2 - scoring of dynamic disciplines [1]

Discipline	Maximum points
Endurance	325
Efficiency	100
Autocross	100
Skidpad	75
Acceleration	75

For each discipline, the hybrid system described in this thesis will be used differently and the main body of this work will be aimed at maximizing points scored in the Endurance event. For this reason, I will shortly describe each discipline.

2.2.1. Acceleration

Acceleration event measures the straight-line acceleration of the vehicle from a standing start. The acceleration track has a fixed length of 75 m and a width of 3 m [1]. Time to complete the track is measured and compared to other teams to assign points.

2.2.2. Skidpad

Skidpad event is aimed at testing the steady-state cornering capability of the vehicle. Skidpad track consists of two circles in a figure eight pattern. The vehicle completes two laps in each circle and the times of the second lap in each are then averaged to provide the final time for this event [1].

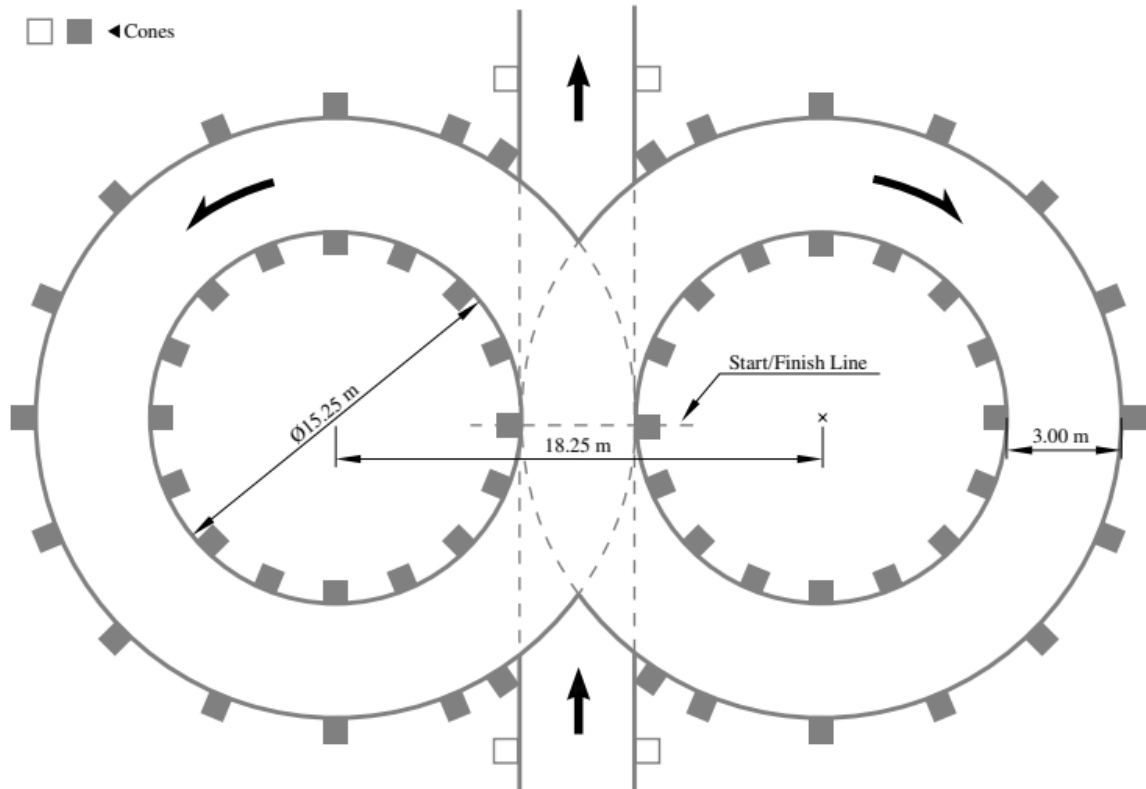


Figure 1 - Skidpad track layout [1]

2.2.3. Autocross

The autocross track layout is built according to guidelines specified by the Formula Student rules, but the shape of the track is specific to each competition event. The track is usually quite technical and consists of short straights, chicanes, decreasing radius turns, etc. The vehicle performs a single measured lap from a standing start and the lap time determines the running order for the Endurance event, where the track is usually the same or very similar.

2.2.4. Endurance and Efficiency

One lap of the endurance track is approximately 1 km long and the length of the complete endurance is approximately 22 km. After the first driver completes 11 km, they will be signaled into the driver change area. The second driver then completes the rest of the race [1].

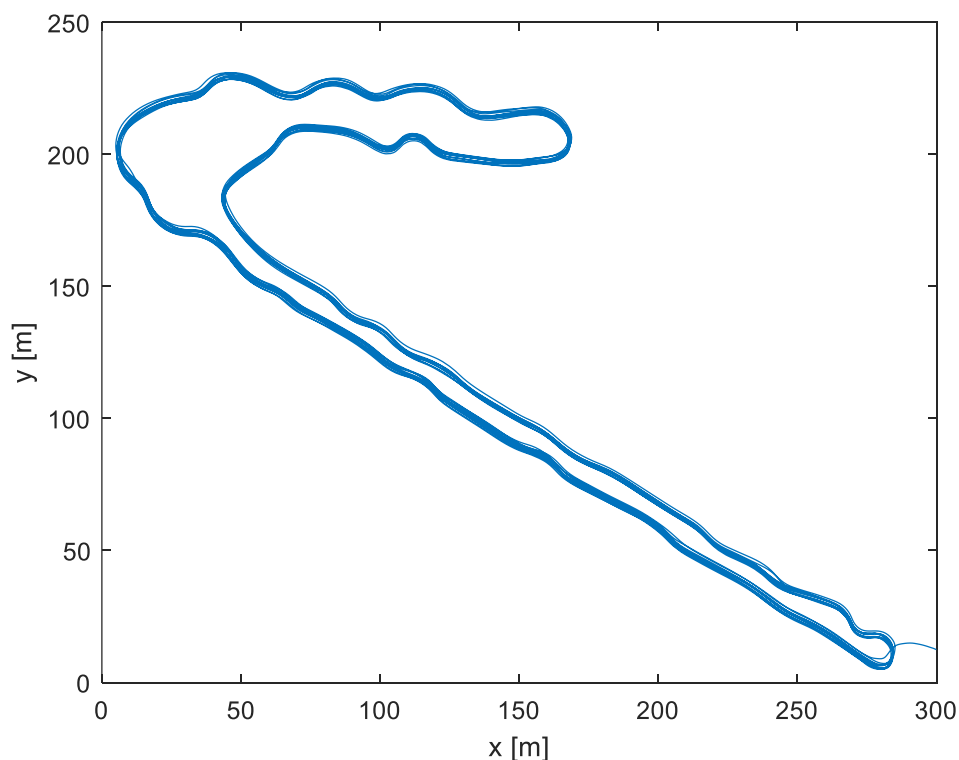


Figure 2 - Formula Student East 2021 Endurance track

After completing the endurance, the fuel consumption is measured by refilling the tank to the starting volume and the measured fuel mass is compared to other teams to assign points for efficiency.

3. HYBRID ELECTRIC VEHICLES

Recent trends in the automotive industry aim at the reduction of greenhouse gas emissions to reduce the impact of transportation on the climate. A growing number of governments have announced aggressive timelines for elimination of internal combustion engine vehicles (ICEVs) [2]. To reduce the emissions on the end vehicle, apart from the production of the energy and manufacturing processes, most leading automakers are shifting their focus from ICEVs to battery electric vehicles (BEVs). The transition from ICEVs to BEVs has not been smooth because of the limitations of the power grid infrastructure in most places and because the battery technology development is still in its early stages. Hybrid electric vehicles (HEVs) have proven to be a necessary bridge into the eventual complete BEV transition [3]. For these reasons, Formula Student competitions decided to allow hybrid powertrains in the combustion category, to give the students the opportunity to explore and exploit opportunities of such systems.

3.1. Main hybrid categorization

HEV powertrains can be classified into three main categories, which are series, parallel and series-parallel split.

In a series hybrid, the engine drives a generator instead of driving the wheels. This generator provides the energy to charge the battery which in turn powers the electric motors driving the wheels. This configuration allows for independent control of the engine speed, thus allowing the ICE to run in its optimal rpm range [4].

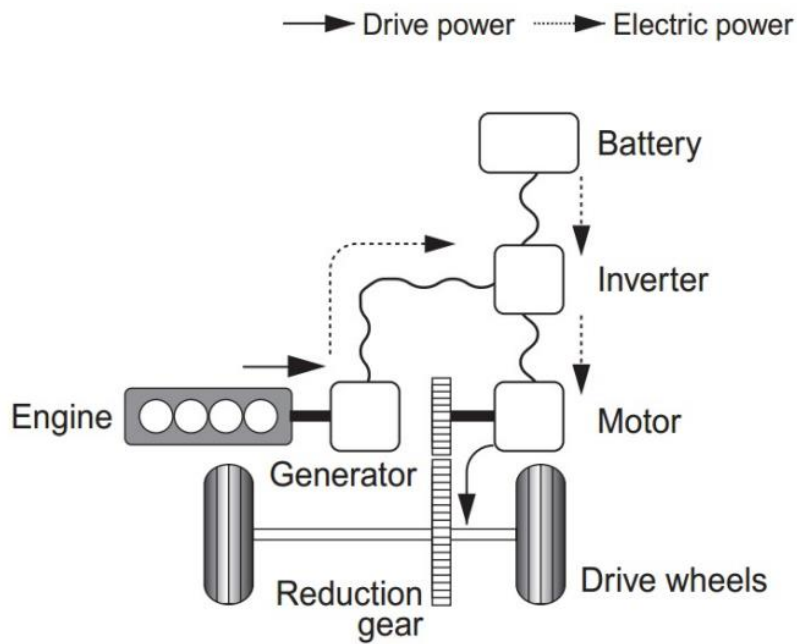


Figure 3 - schematic diagram of series hybrid vehicle [5]

In a parallel hybrid, both the engine and the electric motor drive the wheels, and the drive power obtained from these two sources can be utilized according to the power requirement. The battery can be recharged by the process of regenerative braking and during cruising by the motor acting as a generator when the ICE power produced is more than the power needed for propulsion [5].

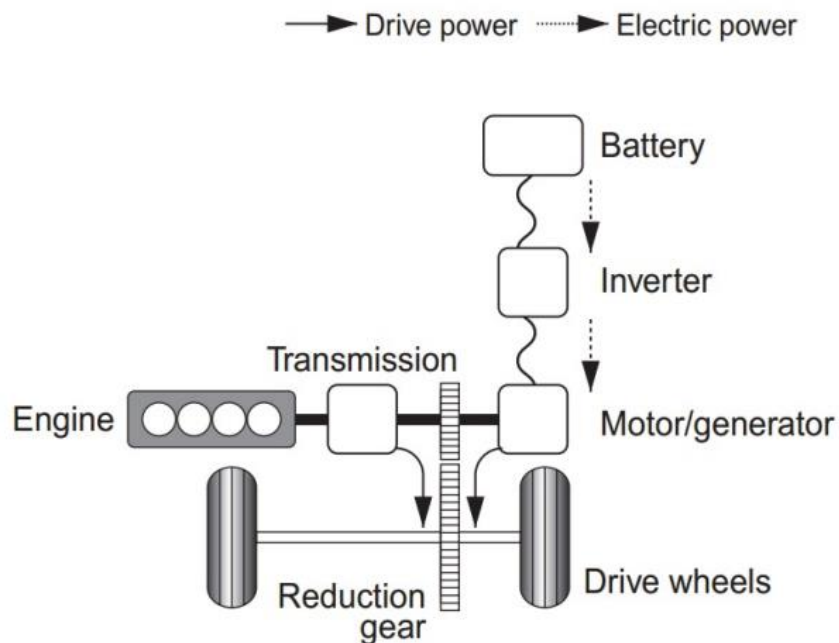


Figure 4 - schematic diagram of parallel hybrid vehicle [5]

A series/parallel hybrid system also known as the power split system is a combination of both previously mentioned architectures. This arrangement allows for more versatile power control and. It also provides an option to drive the wheels while simultaneously generating electricity using a generator. Depending on the driving conditions, the power is extracted from only the electric engine or from both the electric motor and the engine in order to maximize efficiency [5].

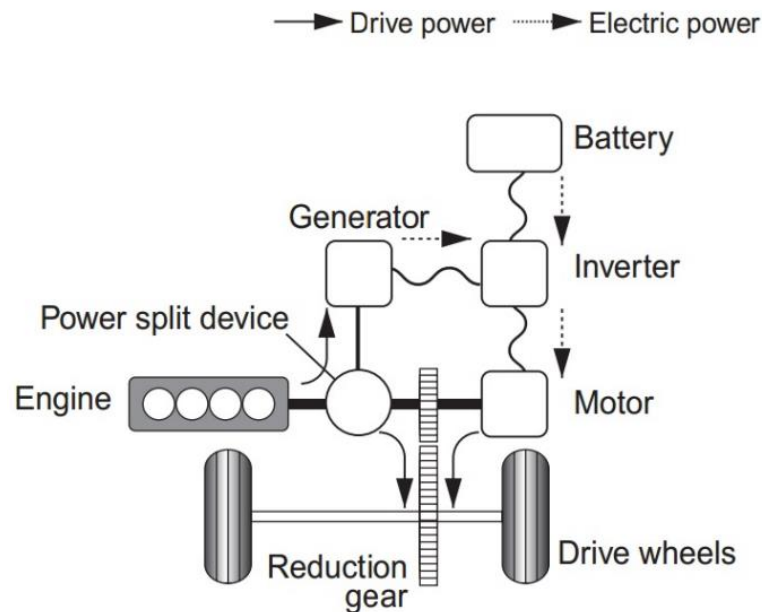


Figure 5 - schematic diagram of series/parallel hybrid vehicle [5]

3.2. Strength categorization

HEVs are further categorized by their voltage, power and extensiveness of utilization, which is sometimes called the strength of the hybrid, because it reflects the overall concept of the implementation of the system.

Table 3 - strength categorization of hybrid vehicles [6]

Parameter	Micro hybrid	Mild hybrid	Full hybrid	Plug-in hybrid
Battery voltage [V]	12	48 – 160	200 – 300	300 – 400
Electric machine power [kW]	2 ... 3	10 ... 15	30 ... 50	60 ... 100

Weaker hybrids usually allow implementation of idle start/stop systems or provide additional torque assistance to fill or boost the torque provided by the ICE.

On the other hand, stronger hybrids can switch to full electric driving and provide substantial electric torque [6].

3.3. Topology categorization

Lastly, mild hybrid electric vehicles (MHEVs) are categorized by the positioning of the main components of the hybrid electric system on the vehicle. This categorization takes into account mainly the position of the electric motor and the type of connection with the powertrain (belt, integrated or gear mesh) [7].

Table 4 - topology categorization of hybrid vehicles [7]

Type	Description
P0	The electric machine is connected with the internal combustion engine through a belt, on the front-end accessory drive (FEAD).
P1	The electric machine is connected directly with the crankshaft of the internal combustion engine.
P2	The electric machine is side-attached (through a belt) or integrated between the internal combustion engine and the transmission; the electric machine is decoupled from the ICE and it has the same speed of the ICE (or multiple of it).
P3	The electric machine is connected through a gear mesh with the transmission; the electric machine is decoupled from the ICE and its speed is a multiple of the wheel speed.
P4	The electric machine is connected through a gear mesh on the axle of the vehicle; the electric machine is decoupled from the ICE and it's located on the axle drive or in the wheel hub.

The differences of each type are best understood from the following figure.

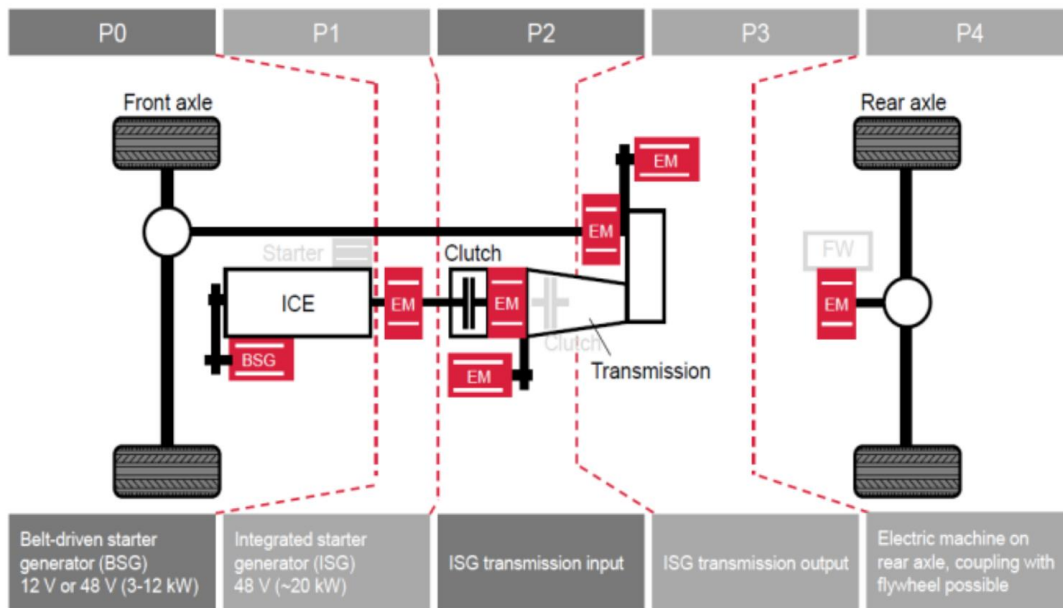


Figure 6 - diagram of different topology types of a MHEV [8]

3.4. Hybrid vehicle energy optimization

Optimization problems focused on the energy consumption of a hybrid vehicle can have various definitions of their objective function. Very often, such optimizations aim at minimizing the total energy consumption on a given trajectory [9], thus maximizing the total range of the vehicle. Other optimizations may minimize the total cost of consumed energy based on different primary sources (electric energy from the grid and fossil fuels) [10]. Yet another approach is to optimize for minimizing the production of exhaust emissions [11] [9]. Most of the contributions to this topic are based on the assumption that the speed and the acceleration of the vehicle are solely determined by the driver and are not influenced by the energy management strategy. Therefore, the authors often use predefined velocity trajectories to conduct their investigations [12]. These solutions are aimed at passenger cars and often realize the energy management by changing the power split between the ICE and the electric motor [9], which in this case is not applicable, because the ICE on FS.14 is controlled by a mechanical throttle.

In contrast to passenger cars and heavy-duty trucks, a race car focuses on vehicle performance and minimum lap time rather than fuel economy [12]. Such optimizations are usually performed globally, i.e., along the whole track, because the same instantaneous power output can have a different impact on the lap time

depending on the position on the track [13]. In a rear wheel driven race car, the optimizations can also be focused on maximizing energy efficiency, however, mostly in a grip limited region of the track (corner exits), where more power couldn't be utilized [14].

Solutions to those optimization problems vary greatly, because each hybrid system is based on a different concept. Some vehicles are able to split the power generation between the different power units, other can manage energy generation in a dedicated generator or even harvest the energy from a turbo. However, an important finding with regards to lap time optimization is the fact, that an increased speed at the beginning of a straight (especially a long straight) most effectively decreases lap time [15].

4. CTU CARTECH FS.14 CONCEPT

The team CTU CarTech was founded in 2007 and since then has produced 14 Formula Student prototypes. The newest of which is the FS.14 which is also one of the first Formula Student cars to implement a hybrid powertrain under the new rule set.



Figure 7 - FS.14 on Acceleration event at FS Czech 2022

The team is based on the Faculty of mechanical engineering of Czech Technical University in Prague. Thanks to the support of the university, the faculty staff and many of its industry partners, it provides an opportunity to engineering students to compete and compare their skills and knowledge with other prestigious universities from around the world. In such competition, CTU CarTech was able, for a brief moment, to reach 6th place in the world ranking of Formula Student combustion category.

4.1. Overall FS.14 concept

The FS.14 has a hybrid chassis consisting of a carbon fiber monocoque and a rear space frame. A light weight aerodynamic package designed for high downforce at low speeds. A double wishbone suspension with decoupled roll-heave damping system.

Table 5 - main parameters of FS.14

Parameter	Value
Wheelbase	1530 mm
Track	1150 mm front / 1100 mm rear
Weight without a driver	206 kg
Static CoG height with a 70 kg driver	253 mm above ground
Coefficient of drag	1.528
Coefficient of lift	-3.871
Reference frontal area	1.0308 m ²

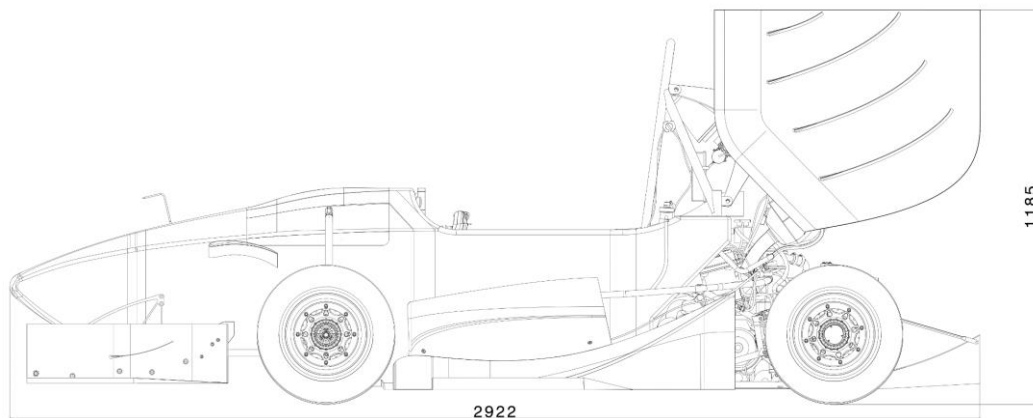


Figure 8 - FS.14 side view

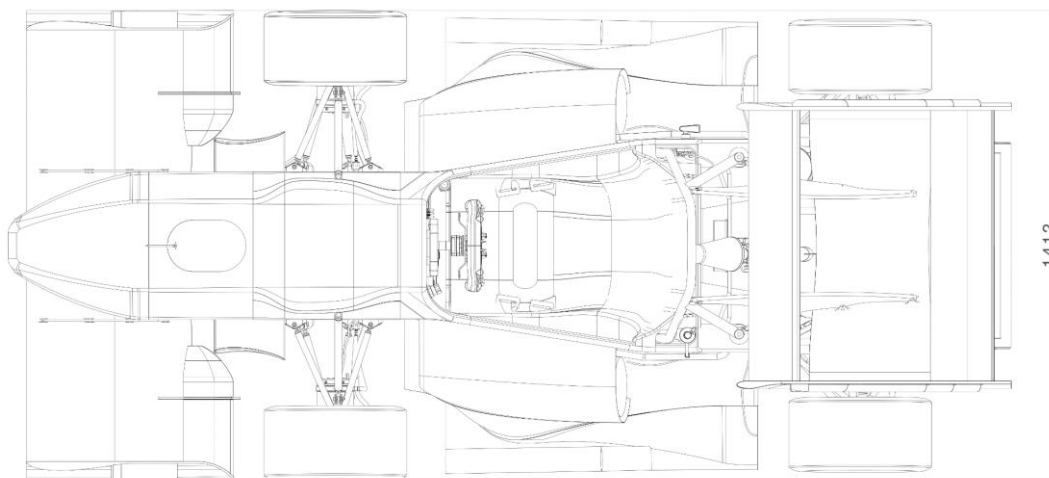


Figure 9 - FS.14 top view

4.2. FS.14 powertrain

The FS.14 has a Yamaha R6 internal combustion engine driving the rear wheels as the main power unit. Secondary hybrid powertrain independently drives the front wheels via in-wheel planetary gearboxes with Plettenberg electric motors.

Table 6 - main parameters of FS.14 powertrain

Parameter	Value
ICE peak power	64 kW at 11000 rpm
ICE peak torque	60 Nm at 11000 rpm
Gear ration in 1 st gear with the final gear	7.7
Hybrid battery nominal voltage	46.2 V
Hybrid battery nominal capacity	230 Wh
Peak hybrid system power	8.5 kW
Peak hybrid torque (combined)	21.4 Nm at 3822 rpm
Hybrid motor gear ratio	5.6

The hybrid vehicle classifies as a parallel mild hybrid with a P4 topology. This concept was chosen mainly to utilize the longitudinal grip on the front axle and to harvest the energy from it during recuperation. Further, independent drive to each of the front wheels opens opportunities for yaw control using torque vectoring.

4.3. Hybrid energy storage

The rules specify, that the maximum weight of the HSC (Hybrid Storage Container) is 3 kg including casing [16]. The chosen cells for the HSC are 26650 Lithium Ion Power Cells from LithiumWerks. The configuration of the battery is 14S 2P (2 cells in parallel and 14 cells in series). This configuration yields the following parameters:

Table 7 - hybrid energy storage parameters

Parameter	Value
Nominal battery voltage	46.2 V
Maximum continuous charge current	20 A
Maximum peak charge current (10s)	40 A
Maximum continuous discharge current	100 A
Maximum peak discharge current (10s)	240 A
Expected power (2s)	8 512 W

The hybrid energy storage is independent from the rest of the systems of the vehicle. Control electronics, the engine control unit, cooling fans and water pumps are powered by an ICEs alternator and a separate battery. The power usage of these systems is closely matched to the power provided by the alternator and any excess energy is dissipated into heat. For this reason, losses from the auxiliary systems won't be further examined in the main body of this thesis.

5. THE FUNDAMENTALS OF RACING

This chapter provides a brief introduction to the theoretical concepts used throughout this work and in the discipline of racing in general. Understanding of concepts like g-g-v diagrams and the phases of cornering is critical for understanding the concepts described in the rest of this thesis.

5.1. The g-g and g-g-v diagram

The g-g diagram describes the cornering, acceleration and deceleration capabilities of a given vehicle regardless of its other parameters. The goal of a racing driver is to spend as much time as possible as close as possible to the potential vehicle g-g boundary [17].

The basic design requirements of a race car are [17]:

- The provision of a largest g-g area throughout the range of operating conditions.
- The provision of vehicle control and stability characteristics that enable a skilled driver to operate at or near these acceleration limits.

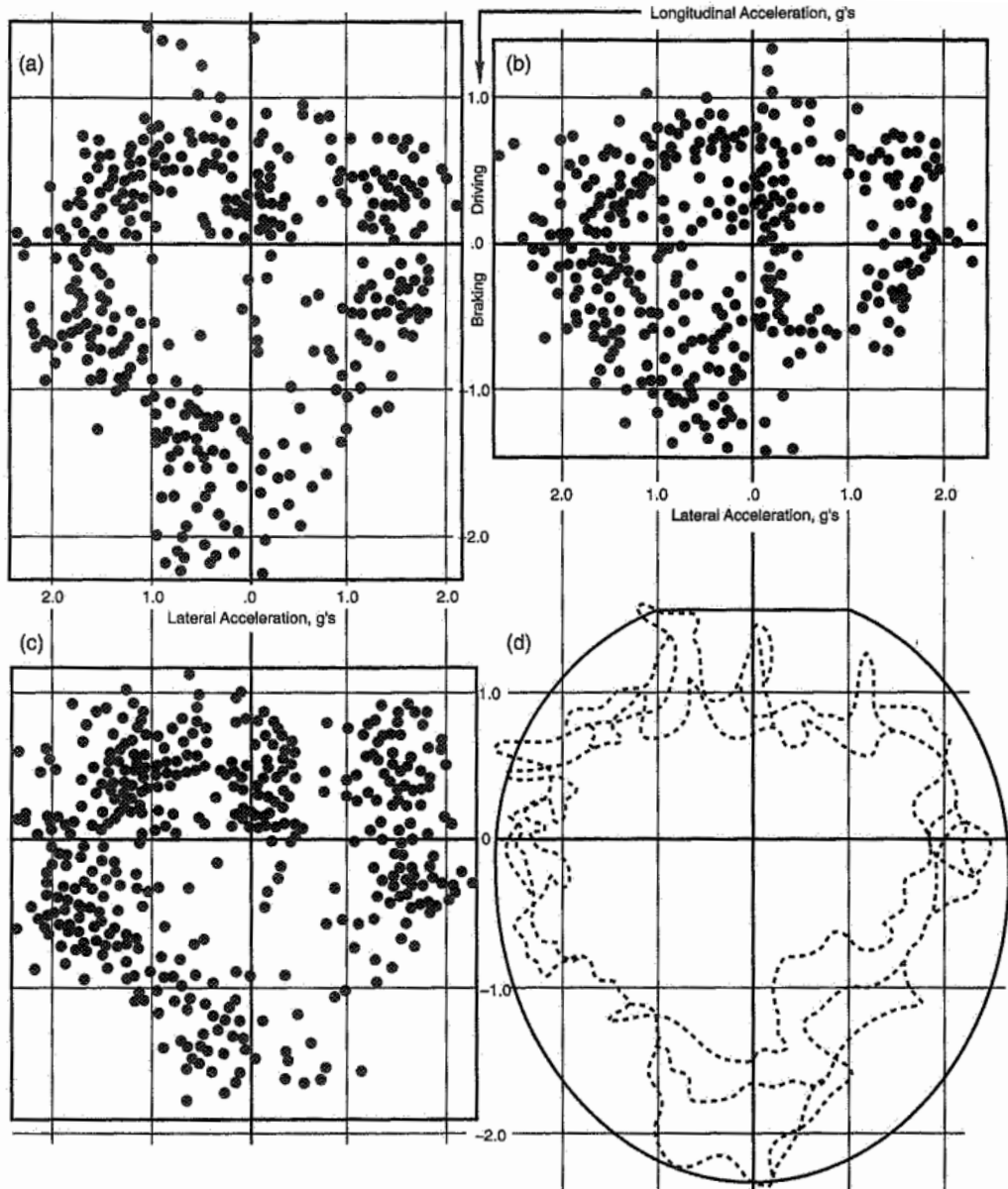


Figure 10 - g-g measurements on a Grand Prix car [17]

The g-g area changes with different operating conditions. For example, for a vehicle generating aerodynamic downforce, higher speeds allow for more grip and therefore more acceleration potential. For this reason, a g-g-v diagram is often used to describe the variability of the acceleration boundary with speed.

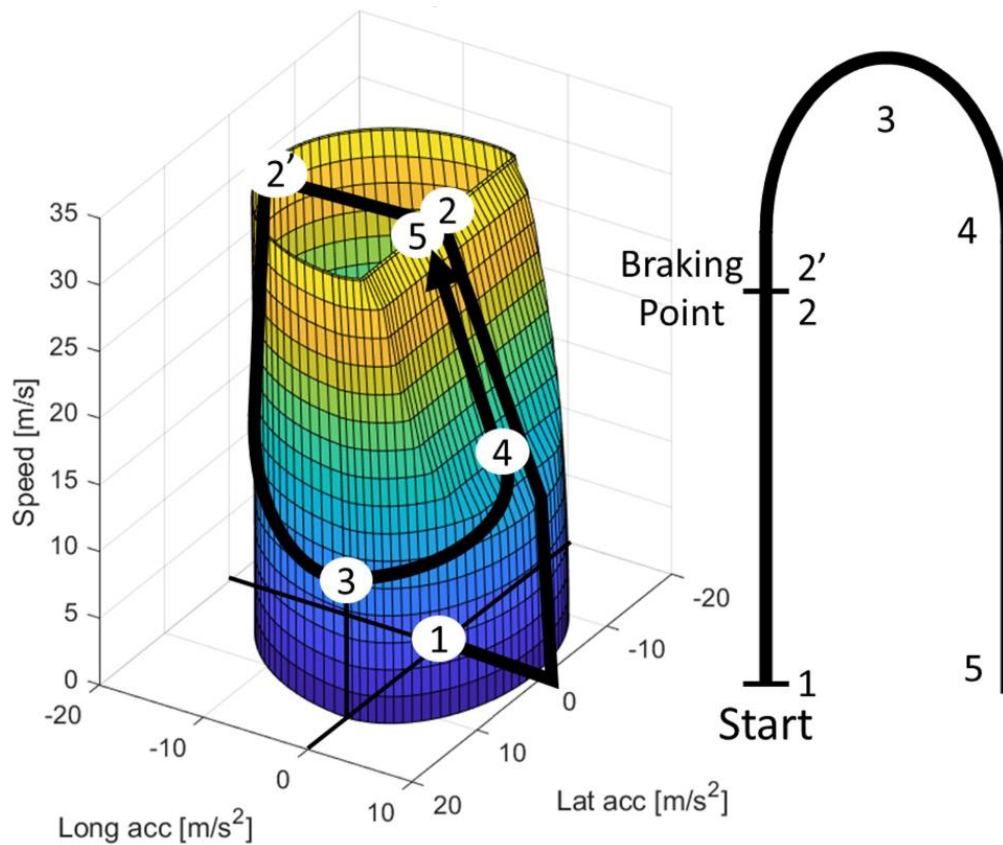


Figure 11 - lateral and longitudinal acceleration versus speed and the progression around the performance envelope [18]

On the figure above, the g-g area can be observed to decrease in size with rising vehicle speed due to a power limitation. In this example the vehicle doesn't generate any aerodynamic downforce, therefore the area doesn't expand.

5.2. Phases of cornering

Cornering maneuver on a race track can be divided into 5 main phases:

1. Pure braking

The vehicle uses its whole longitudinal friction potential for deceleration to achieve the corner entry speed as quickly as possible.

2. Combined braking and cornering (corner entry, trail braking)

In the next phase, the vehicle begins to rotate into the corner while still decelerating. A part of the friction potential for braking is sacrificed to generate forces to start the rotation of the vehicle.

3. Steady state cornering

The vehicle already achieved the desired yaw rate and now corners with using all of its lateral friction potential for cornering.

4. Combined acceleration and cornering (corner exit)

The lateral friction decreases and the difference between the front and rear lateral forces is used to slow down the rotation of the vehicle. Part of the cornering ability of the tires is sacrificed to allow for the start of acceleration for the next straight.

5. Pure acceleration

In the last phase, all of the friction potential of the vehicle is used for acceleration.

In the context of g-g diagrams, these phases can be better understood with the following illustration.

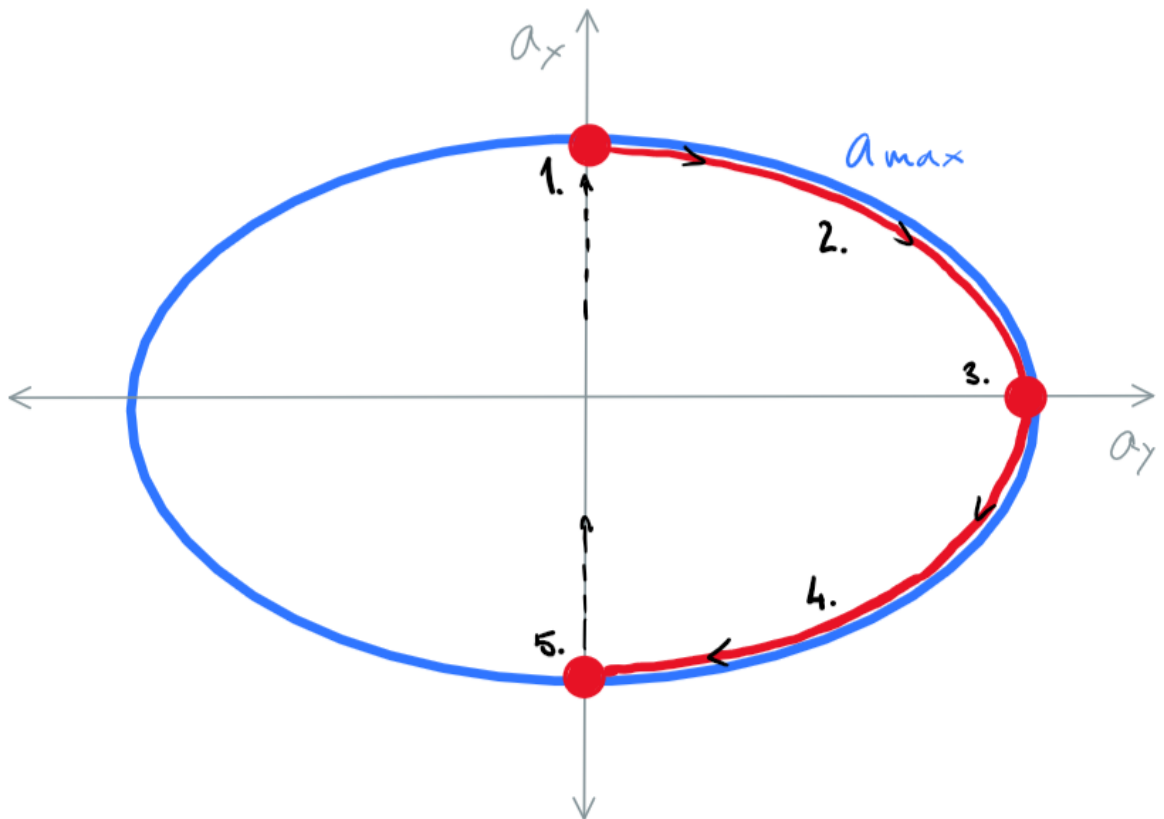


Figure 12 - illustration of the cornering phases on a g-g diagram

6. LAP TIME SIMULATIONS

When developing a race car, lap time simulations become a crucial input in decision making. The overall objective of a race car is to win a race. Depending on a racing series, the complexity of such a goal can differ. For example, in a Formula 1 series, the success in a single race depends on the pit-stop strategy and tire choice, vehicle setup for the particular track, strategies and the track positions of the opponents, reliability of the vehicle and of course, the performance of the driver. An F1 race can be further made more unpredictable by an accident and deployment of a safety car or a sudden change in the weather.

Thanks to the nature of the Formula Student regulations, many of such unpredictable factors are eliminated and the performance of a car becomes more dependent on the design of the car. It could be argued that the success is more in the hands of the engineers than in the hands of the driver when compared to most other motorsport series.

Furthermore, as mentioned before, the objective of a Formula Student event is not simply to win a race, but rather to score the most points. Since there are five dynamic disciplines in which the car performance is measured and scored, it is not as simple as making the car as fast as possible, because the parameters of the car affect performance in each of the disciplines differently. For example, if a car was to be designed for the Acceleration discipline, it would have as little aerodynamic drag as possible while at the same time sacrificing unnecessary downforce. It would have large rear tires to maximize traction and smaller front tires to minimize mass. Such car, however, would likely perform rather poorly in Skidpad. Therefore, the car has to be designed with all the dynamic disciplines in mind and the goal of such car should be to maximize the sum of points in these disciplines. For this reason, a lap time simulation for Formula Student should evaluate the car performance in each of the disciplines.

6.1. The current Lap Time simulations used in CTU CarTech

To better understand the basic characteristics of each vehicle and to objectively set development goals for the next season, CTU CarTech uses the OptimumLap simulation. OptimumLap is a steady state point mass simulation and as such is only capable to evaluate a few key parameters of the car.

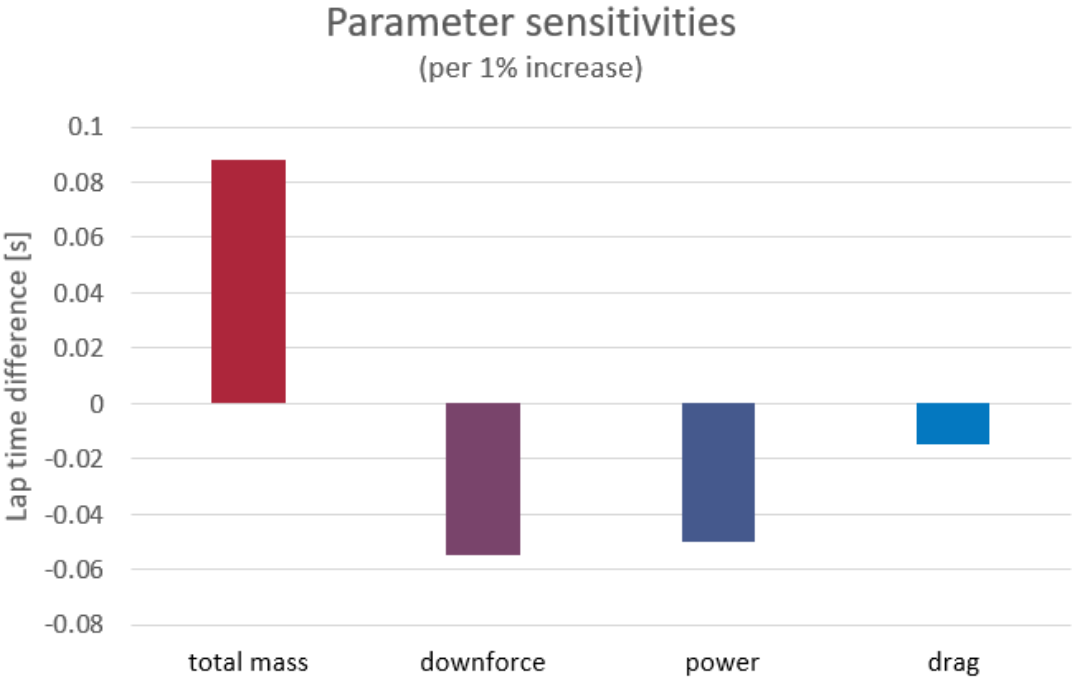


Figure 13 - lap time sensitivities of FS.13 as simulated in OptimumLap

Such analysis is useful for estimation of the effects of increasing power, saving mass or deciding how much drag the aerodynamicists can afford for an improvement of downforce when designing a new aerodynamic feature. However, for more complex analysis, as will be examined in this thesis, this is not sufficient. To evaluate the effects of the height of the center of gravity, the yaw inertia, the influence of active aerodynamic devices, and most importantly for this case, the influence of additional independent drive on the front axle and its energy usage, a lap time simulation with a more complex vehicle model with a certain degree of customizability must be used.

There is a range of different methods for performing lap time simulations, each with different complexity of the model and different assumptions made when

designing the vehicle model. Each has its strengths and weaknesses which will be examined in the following chapters.

6.2. Steady state method

Steady state lap time simulation uses a simple model of a track composed of straights and simple corners (arcs with a constant radius). The model of the vehicle is a point mass with assigned maximal lateral and longitudinal acceleration. The accelerations can be defined as functions of other parameters such as speed (to take aerodynamics or maximum power into account).

The cornering speed for a curved section of the track is calculated using the following formula.

$$v_{R(i)} = \sqrt{\frac{a_y}{R_i}} \tag{6.1}$$

where $v_{R(i)}$ is the speed for a given corner section of the track; a_y is the maximal lateral acceleration at such speed and R_i is the radius of the given section.

Each straight section is then divided into two sections in a way, that the vehicle accelerates from the previous corner using the maximal tractive acceleration and starts braking with the maximal braking acceleration just in time to slow down to enter the next corner.

The accuracy of this method depends on the correct model of the track and a good estimate of the acceleration capabilities of the vehicle, but other parameters are ignored. This method, while being almost trivial enough to calculate even on paper, has a considerable drawback, for example for the calculation of energy consumption, since it omits the combined phases of cornering. A real car (with an ideal driver) brakes in the corner entry until the lateral capabilities of the tire are fully used and there is no traction left for braking. Similarly, on corner exit the driver slowly applies throttle until the full tractive acceleration can be used.

6.3. Quasi-static and quasi-transient methods

This method differs from a steady state lap time simulation in a more accurate model of the track (corners don't have constant radii) and therefore a realistic cornering maneuver with the three phases (trail braking, steady state cornering and combined acceleration and cornering) can be simulated.

6.4. Transient method

The quasi-static and steady state methods work under the assumption, that the vehicle's traction ellipse is always utilized on its maximal potential. In reality, however, a time response of the system must be taken into account. The term "transient effect" refers firstly to the yaw moments, however, there are also other time dependent effects that affect the performance on track. Such effect are, for example, the roll and pitch of the vehicle and the aerodynamic forces resulting from the different position of the chassis or even the tire behavior has a time response. Transient methods generally require a complex vehicle model and often suffer a bad numerical stability [19]. To find the minimal lap time using the transient methods, the task is usually formulated as an optimization problem. The lap time is defined as the objective function and input parameters (drivers inputs) are then found with direct numerical methods. Such computations are often numerically unstable due to strong non-linear tire behavior and significantly more costly. The numerical cost of one lap in Monza is within the range of 24 hours. This fact clearly disqualifies transient methods from the use in further optimization problems, as those could easily take years to perform.

6.5. Choice of a suitable Lap Time simulation

For this project, the following criteria are critical when choosing a Lap Time simulation.

Customizable

For the application in a field as specific as Formula Student with various disciplines and unconventional powertrains, it is necessary to adjust the models frequently (possibly each season) and extensively. An ideal tool on which to base this work would be a simulation made in Matlab Simulink with a good documentation.

Computation time

Since this work aims to use the lap time as an objective function in an optimization problem, it is necessary for the whole simulation to be completed in the order of seconds or minutes, since many iterations will be required. This criterion disqualifies the transient methods from the use in this project.

Accuracy

The optimization problem will depend on the energy consumption (and energy regeneration) of the hybrid powertrain of the vehicle. Further, the concept of the vehicle is aiming at utilizing the additional grip on the front axle in the corner exits by placing electric motors on the front, originally not driven, axle. For this reason, the Steady state method, which omits the combined phases of cornering, is not suitable for this application.

6.6. Choice of a simulation

There are many lap time simulations on the market (or even open source), such as OptimumLap, Chassis Sim or OpenLap, each of which vary in the complexity of the track or the vehicle. By far, however, the most important feature of a simulation for this work is customizability. Since no commercially available lap time simulation offers a satisfactory freedom of customization, I chose a software programmed in Matlab Simulink designed by Ing. Tomáš Novotný as a basis for this project. This simulation software is using the quasi-static method with a pre-calculated traction ellipse and was conceived as a tool for evaluating vehicle performance on a particular track in a form of elapsed time and energy consumption. In the next chapter I will describe the original state of Ing. Novotný's work [20] to give a detailed description of the starting point of my project.

7. LAPTIME TOOL DESCRIPTION

The workflow of the simulation model is divided into two stages.

7.1. Stage I – Initial velocity profile

Stage one of the simulation uses the track and tire data to estimate the velocity profile of the racing lap. This velocity profile is a theoretical speed boundary only considering the adhesion limits of the tires and the track. Powertrain performance will not affect this part of the calculation.

7.1.1. Track analysis

The simulation uses a fixed trajectory defined by XYZ coordinates (or XY in some cases). This method is especially useful for a relatively quick analysis of various tracks obtained directly from the GPS data recorded during the race or during testing.

GPS data conversion

In a case, when the dataset is indeed obtained straight from the GPS device the dataset must be converted into Cartesian coordinates, since the GPS records the terrestrial position, by convention, in height h and two angles, latitude λ and longitude φ . The raw data from the GPS device can then be converted using the following formulas:

$$x = r \cdot \lambda \cdot \cos \varphi \tag{7.1}$$

$$y = r \cdot \varphi \tag{7.2}$$

$$z = h \tag{7.3}$$

where r is the Earth's radius.

Qualitative track description

From the obtained $[xy]$ dataset, the course angle ψ and the track curvature ρ will be calculated using the following formulas:

$$\psi = \tan^{-1} \frac{\Delta y}{\Delta x} \quad (7.4)$$

$$\rho = \frac{\Delta \psi}{\Delta s} \quad (7.5)$$

where Δs is the distance of a step. The accuracy of the result depends on the density of trajectory points.

The points P_i and $P_{i+\Delta}$ are points chosen from the dataset determined by the step size Δ . To ensure there is always a midpoint between the two points P_i and $P_{i+\Delta}$, the step size must be an odd integer higher than 2.

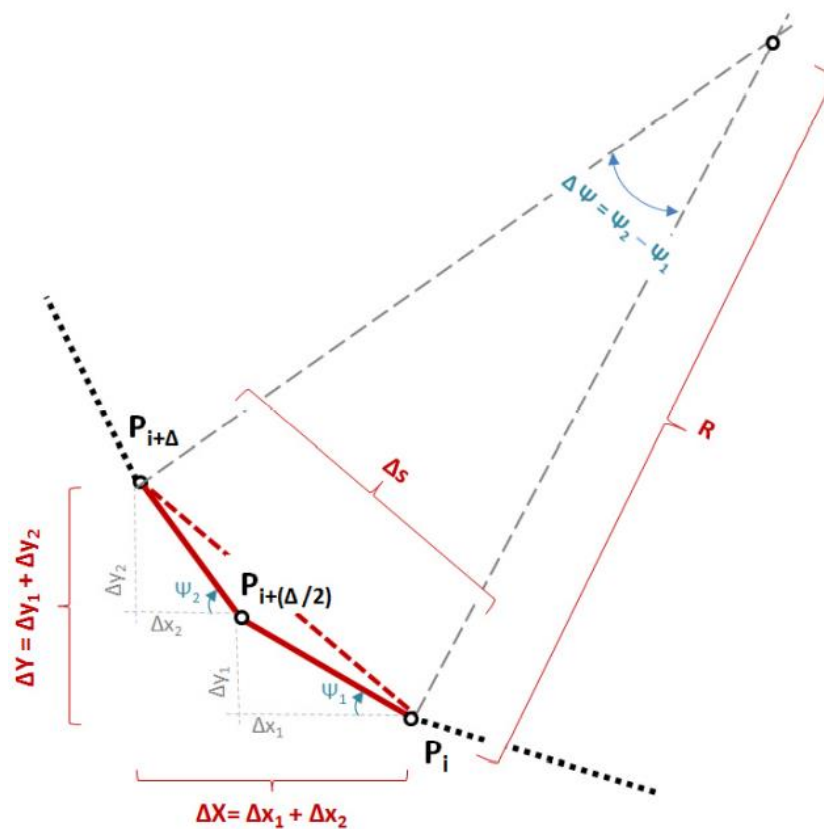


Figure 14 - track analysis [20]

Filtering and smoothing

All resulting data points are continuously connected and occasional out of range peaks are eliminated.

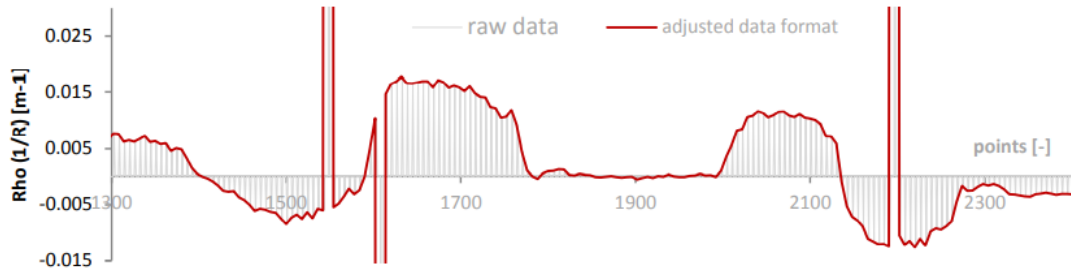


Figure 15 - Data filtering - step 1 [20]

Such track profile is then smoothed using the Smooth function (lowess function) from Matlab's Curve Fitting Toolbox.

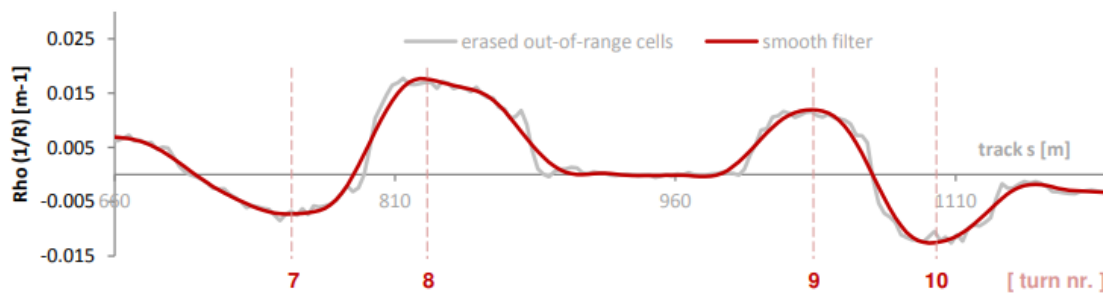


Figure 16 - Data filtering - step 2 [20]

7.1.2. Vehicle performance envelope

The vehicle performance envelope can be described as maximal adhesion limits dependent on speed. The construction of an accurate g-g (or in this case g-g-v) diagram only from the parameters of the vehicle is a complex task requiring a 4-wheel model involving the kinematics and compliances of suspension, a detailed description of the vehicle's aerodynamics (in all dynamic states of the vehicle) and a correct implementation of other effects such as the influence of load transfer and brake balance.

However, there are two variables that affect the g-g-v boundaries the most – the aerodynamic downforce and the tire grip. With an increasing speed, the aerodynamic downforce rises and improves the overall size of the g-g diagram, while rising drag forces increase the power needed to drive the vehicle and

improve braking performance. A simplified model which can later be compared to a real performance of the vehicle for validation should therefore be satisfactory.

Vehicle model:

The vehicle model is a single-track model with the following parameters:

- Static weight distribution
- Implementation of aerodynamic forces (represented by the lift and drag coefficients)
- Non-linear description of tire behavior

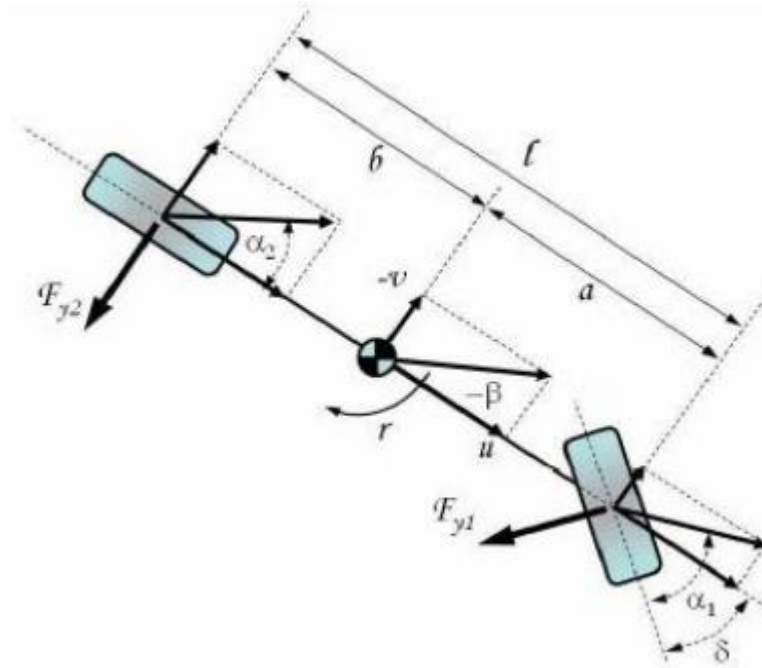


Figure 17 - Single-track model [20]

The equations of motion for a single-track model:

$$m(\dot{v} + u \cdot r) = F_{y1} + F_{y2} \tag{7.6}$$

$$J_z \cdot \dot{r} = a \cdot F_{y1} - b \cdot F_{y2} \tag{7.7}$$

The lateral forces F_{y1} and F_{y2} are obtained from a non-linear tire model PAC2002 based on Pacejka's Magic formula. The lateral forces are a function of front and rear tire loads F_{z1} and F_{z2} and slip angles α_1 and α_2 .

Slip angles:

$$\alpha_1 = \delta - \frac{v + a \cdot r}{u} \quad (7.8)$$

$$\alpha_2 = -\frac{v - b \cdot r}{u} \quad (7.9)$$

Tire loads (static and aerodynamic forces):

$$F_{z1} = m \cdot g \cdot \frac{b}{l} + A \cdot C_{l1} \cdot \frac{\rho}{2} \cdot u^2 \quad (7.10)$$

$$F_{z1} = m \cdot g \cdot \frac{b}{l} + A \cdot C_{l1} \cdot \frac{\rho}{2} \cdot u^2 \quad (7.11)$$

Evaluation strategy of performance envelope:

The single-track model provides simple simulations of a steady-state cornering maneuver in order to obtain maximal values of lateral acceleration at different speeds. This model is then run through a cornering maneuver inspired by NHTSA's routine called SIS (Slowly Increasing Steer) maneuver. Originally, the test is defined by SAE J266 as a test with constant speed and variable steer, for the purposes of the lap time simulation, it has been slightly modified (gray line).

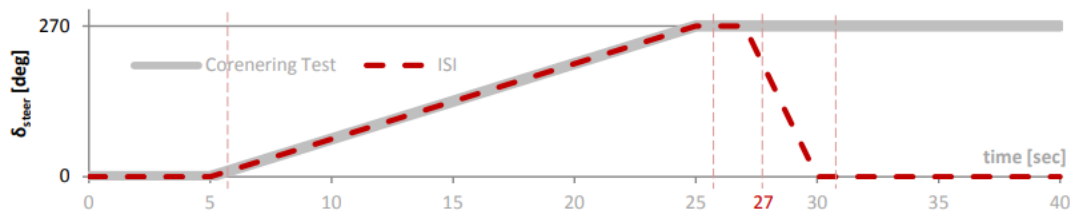


Figure 18 - Slowly increasing maneuver [20]

Final g-g-v diagram is then constructed from the results of this test at various speeds under the assumption that the g-g diagram at each speed takes the shape of a friction circle.

7.1.3. Initial velocity profile

The speed profile described in this section represents the theoretical maximal velocity that satisfies the adhesion limits of the track and the vehicle. This profile is calculated by examining each segment of the track and finding the maximal possible speed that satisfies the constraints of the g-g-v diagram described in the previous chapter. The profile is constructed in four steps.

Step 1 – initial guess

In the first step the maximal cornering speed is calculated for every point N on the track. The maximal cornering speed is a function of the track curvature ρ at that point and the maximal lateral acceleration a_{y_max} . Maximal speed is further constrained by a parameter v_{max} .

$$v_{step1(n)} = \min \left(v_{max}, \sqrt{\frac{a_{y_max}}{\rho(n)}} \right), n = 1 \dots N$$

(7.12)

Since the maximal lateral acceleration a_{y_max} is a function of speed due to aerodynamic forces, the final speed for every point must be iteratively recalculated.

Step 2 – braking phase

The initial guess contains extremely high speed gradients. In this step, the speed gradients will be adjusted to correspond to the maximal longitudinal acceleration a_x from the g-g-v diagram. Each local minimum in the velocity profile represents a critical cornering speed (point $s_{(i)}$). In those circumstances the lateral acceleration capacity is saturated ($a_y = a_{y_max}$). At that point, no longitudinal acceleration can be performed. In the next point on the track (going backwards $s_{(i-1)}$), under the assumption of a fixed speed ($v_{(i)} = v_{(i-1)}$) and changing curvature ($\rho_{(i-1)} < \rho_{(i)}$), the lateral acceleration capacity will not be fully saturated and therefore the vehicle can decelerate with the maximal available longitudinal acceleration.

for $i = 1 \dots N$

$$a_{y(i-1)} = v_{step1(i)}^2 \cdot \rho(i)$$

(7.13)

$$a_{x_brake(i-1)} = \sqrt{\left(1 - \frac{a_{y(i-1)}^2}{a_{y_max}^2}\right) \cdot a_{x_max}^2} \quad (7.14)$$

$$v_{(i-1)} = \sqrt{v_{step1(i)}^2 + 2 \cdot a_{x_brake(i-1)} \cdot \Delta s} \quad (7.15)$$

Since also in this case, aerodynamic forces play a substantial role and are a function of speed, the calculation for each point has to be iterated.

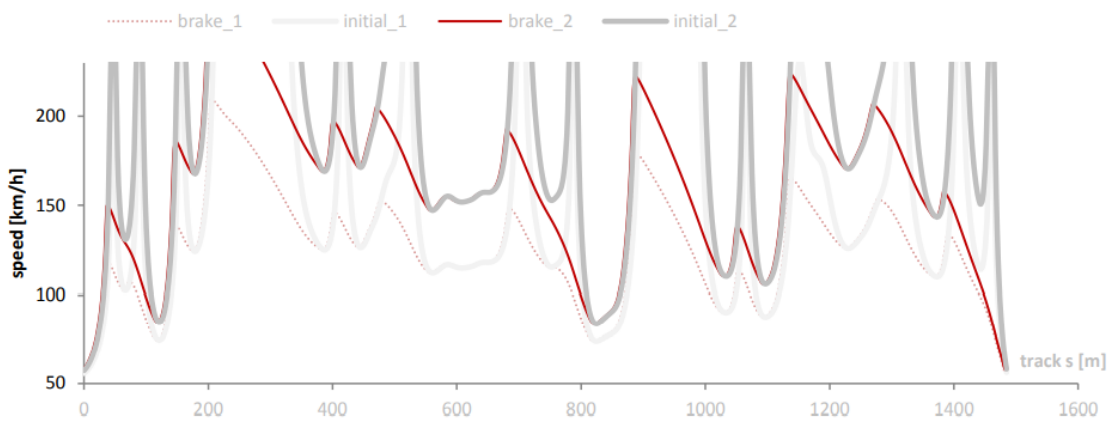


Figure 19 - corrected speed estimate - braking phase [20]

Step 3 – accelerating phase

The same principle as for braking in step 2 is used for acceleration only in different direction. The limitations of the powertrain are not taken into account, therefore, the same longitudinal acceleration capacity can be used. The power limitations and other factors influencing longitudinal dynamics will be simulated in the stage II of the simulation.

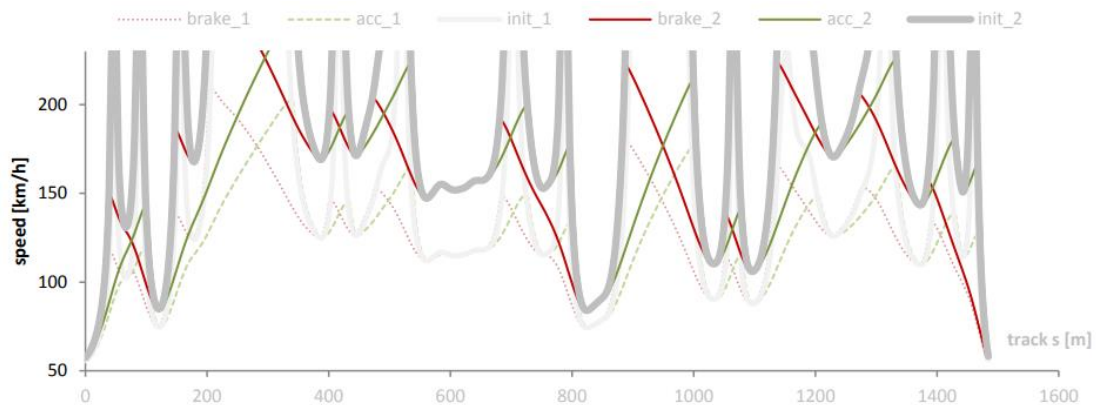


Figure 20 - corrected speed estimate - accelerating and braking [20]

Step 4 – correction of the velocity profile

In the last steps, previously calculated parts of the velocity profile are connected into one.

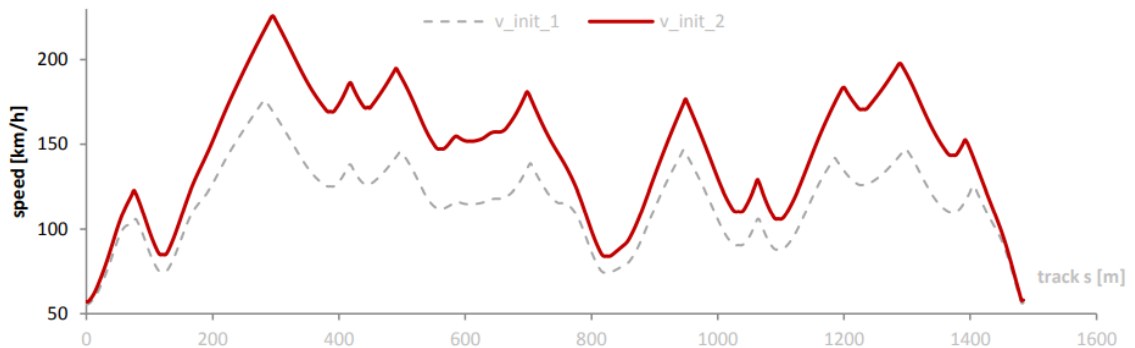


Figure 21 - boundary velocity profile [20]

The difference from real velocity profiles is obvious at first look. Speed gradients during acceleration and braking differ greatly in real cases. This initial profile represents a boundary of an operational area (or the target values) for the longitudinal speed controller in stage II of the simulation.

7.2. Stage II – Simulation model

The aim of the second stage of the simulation is to perform a model-based simulation of the final racing time of the track analyzed in stage I and perform an estimation of consumed fuel. During the simulation a closed-loop controller measures a difference between the achieved speed by the powertrain model and the initial velocity profile. Based on the measured difference a PI controller decides whether to brake or accelerate and by how much. These two values (brake and throttle pedal values) serve as inputs into the powertrain model.

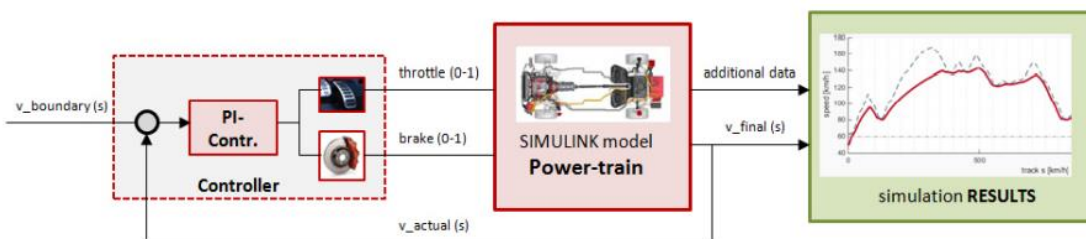


Figure 22 - simulation model - Stage II [20]

7.2.1. Powertrain model

The model of a powertrain is a rigid model of longitudinal dynamics. The inputs for the model are the throttle position and the actual angular speed of the engine ω_E . The output of this model is the driving force F_x .



Figure 23 - schematic powertrain Simulink model [20]

The ICE (internal combustion engine) in this model is represented by a lookup table of values of torque at different engine speeds as measured on a test bench.

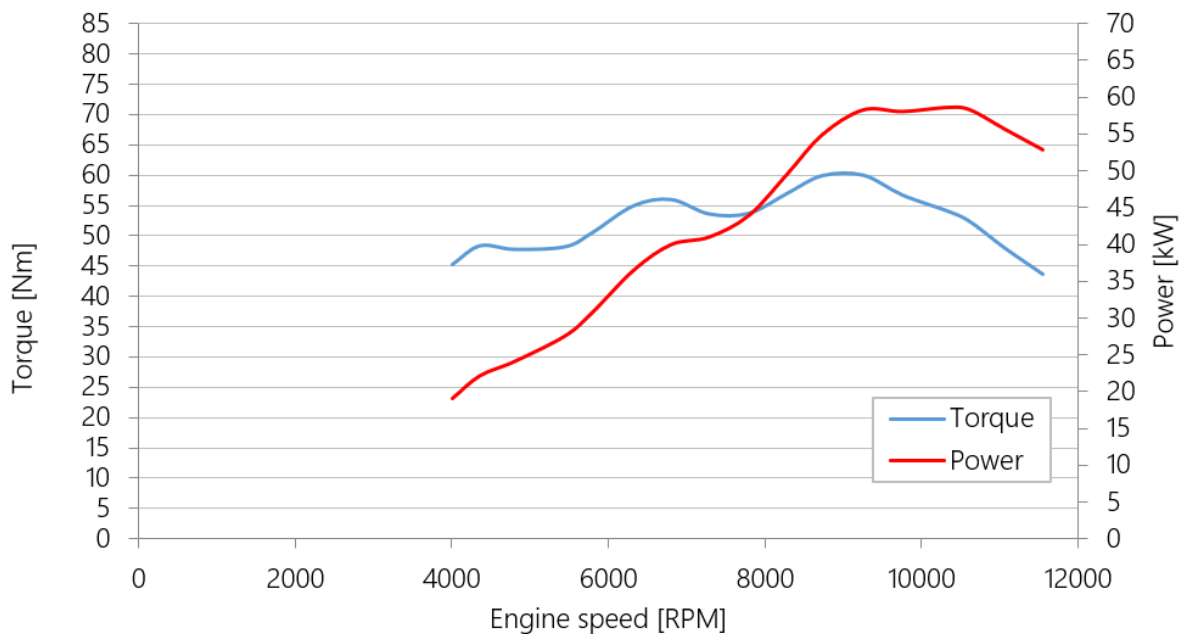


Figure 24 - torque and power characteristic of a modified Yamaha R6 engine used on FS.14 [21]

The resulting torque is then multiplied by a transmission ratio that depends on the current gear. The transmission block simply chooses a gear based on the current engine rpm. Thresholds for upshifts and downshifts as well as ratios of every gear are input variables different for each vehicle.

7.2.2. Longitudinal dynamics

The resulting force on the vehicle F_{net} of the vehicle is determined by the regulated driving force F_D of the powertrain, regulated braking force F_B and other forces acting on the vehicle, such as the total rolling resistance of all four wheels F_R , the climbing resistance F_C , the air resistance F_A and the inertial resistance F_I . Braking force is modeled as a liner function of the brake pedal input.

$$F_{net} = F_D - F_B - F_R - F_C - F_A - F_I \quad (7.16)$$

$$F_D = F_D(throttle, \omega_E) \quad (7.17)$$

$$F_B = F_B(brake) \quad (7.18)$$

$$F_R = k_R \cdot F_Z \quad (7.19)$$

$$F_C = m_v \cdot g \cdot \sin(\alpha_{sl}) \quad (7.20)$$

$$F_A = A \cdot C_d \cdot \frac{\rho}{2} \cdot v^2 \quad (7.21)$$

$$F_I = F_{I,trans} + F_{I,rot} = \left(m_v + \frac{J_{red,i_g}}{r_{dyn}^2} \right) \cdot a_x \quad (7.22)$$

Inertial resistance takes into account the reduced moment of inertia of the whole vehicle for an engaged gear.

$$J_{red,i_g} = 4 \cdot J_W + i_{diff}^2 \cdot J_{Dr} + i_{g(i)}^2 \cdot i_{diff}^2 \cdot (J_E + J_C + J_G) \quad (7.23)$$

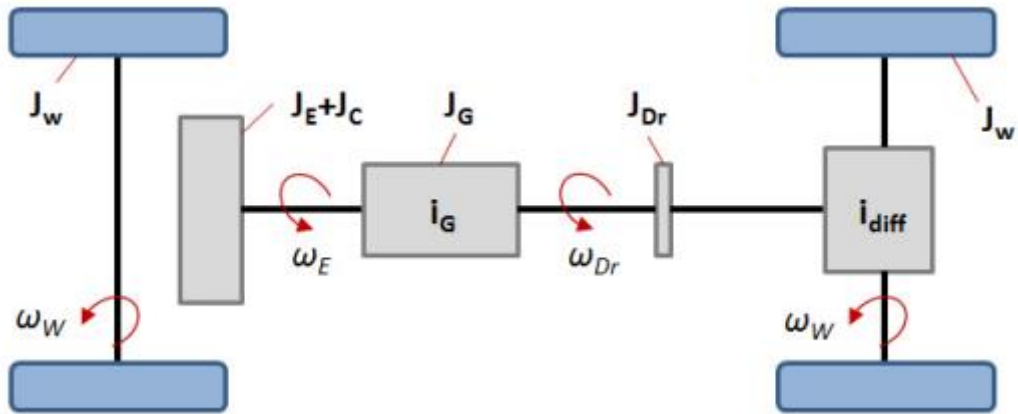


Figure 25 - schematic powertrain model [20]

To obtain the desired result – speed, the equations are formulated in the following way.

$$a_x = \ddot{s} = \frac{F_{net}}{m_{red}} \tag{7.24}$$

$$v = \dot{s} = \int \frac{F_{net}}{m_{red}} dt \tag{7.25}$$

7.2.3. Fuel consumption

Fuel consumption analysis is based on a BSFC map (brake specific fuel consumption) of the chosen engine. Once we know the working point of the engine (n, p_e), the BSFC map gives us an estimate of the specific fuel consumption b_e in g/kWh . The integral of all state points over the whole time interval gives us the total fuel consumption.

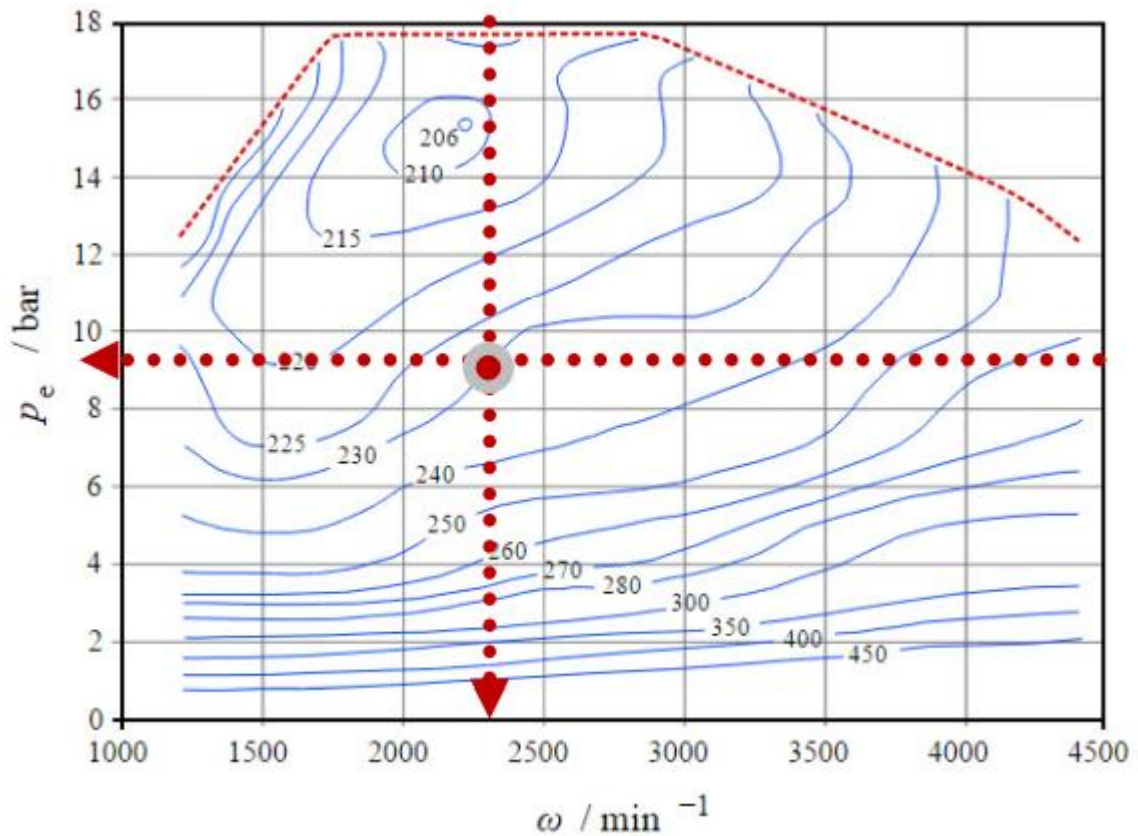


Figure 26 - BSFC map [20]

8. LAPTIME TOOL ADJUSTMENT

The concept of FS.14 is different than conventional road vehicles for which the lap time simulation was originally designed. For that reason, a few adjustments to the Ing. Novotný's simulation will need to be realized.

8.1. Tire model

The original single-track only models the lateral dynamics of the tire. Since our new single-track model with front wheel drive operates with the longitudinal tire forces, this won't be sufficient. Originally, the simulation model uses the lateral tire characteristics represented in Pacejka's tire model PAC2002. This model could also be used for longitudinal dynamics, however, tire testing data for longitudinal dynamics of the tires chosen for FS.14 are not available, therefore, I must choose an empirical approach. In the next two chapters I will describe modeling of longitudinal and lateral dynamics of Hoosier 16" R25B tires.

8.1.1. Lateral tire dynamics

For lateral dynamics, Pacejka's tire model PAC2002 will be used and the same method for determining the lateral part of the g-g-v diagram as in the original work [20] will be used. Detail of that were already described in chapter 7.

8.1.2. Longitudinal tire dynamics

Tire testing is an expensive and complicated process. Since there is a wide and still growing supply of available tire choices for Formula Student, testing each tire to make an educated choice wouldn't be conceivable for most of the teams due to limited resources. For this reason, a volunteer-managed organization called FSAE Tire Test Consortium conducts testing of these tires for member schools which pool their resources.

On the chosen tire, Hoosier 16" R25B, due to its dimensions, longitudinal dynamics couldn't be tested however. For this reason, an empirical method for basic modeling must be used. The aim of the tire model is to determine the shape of the g-g-v diagram. Usually, the data from inertial sensors on the vehicle could be sufficient, however, in this case I aim to evaluate the added benefit of traction on the front axle. Since all previous vehicles of CTU CarTech team were rear wheel driven, no such data, that would represent the new concept are available. Theoretically, longitudinal acceleration measured during braking should be similar to the full potential of the 4WD acceleration, however, peak values of braking acceleration occur at higher speeds due to aerodynamic effects, therefore using the same values for acceleration from standstill would bias the results.

Firstly, I will estimate the longitudinal coefficient of friction f_x of the tires by evaluating the data from the Acceleration discipline. In this discipline, the car accelerates from a standstill, therefore aerodynamic affects (both on tire load and weight transfer) can be neglected. From the peak acceleration measured in that discipline and the mass of the vehicle, the coefficient can be estimated simply by the following equation.

$$f_x = \frac{m \cdot a_x}{2F_{z, rear}} \quad (8.1)$$

where m is the mass of the vehicle; a_x is the measure acceleration and F_z is the vertical force.

To get the vertical load on each of the rear tires $F_{z, rear}$, the longitudinal weight transfer due to acceleration must be taken into account. In the calculation, since this is a quasi-static simulation, I will neglect the transient effects of the sprung mass movement (as explained in chapter 6).

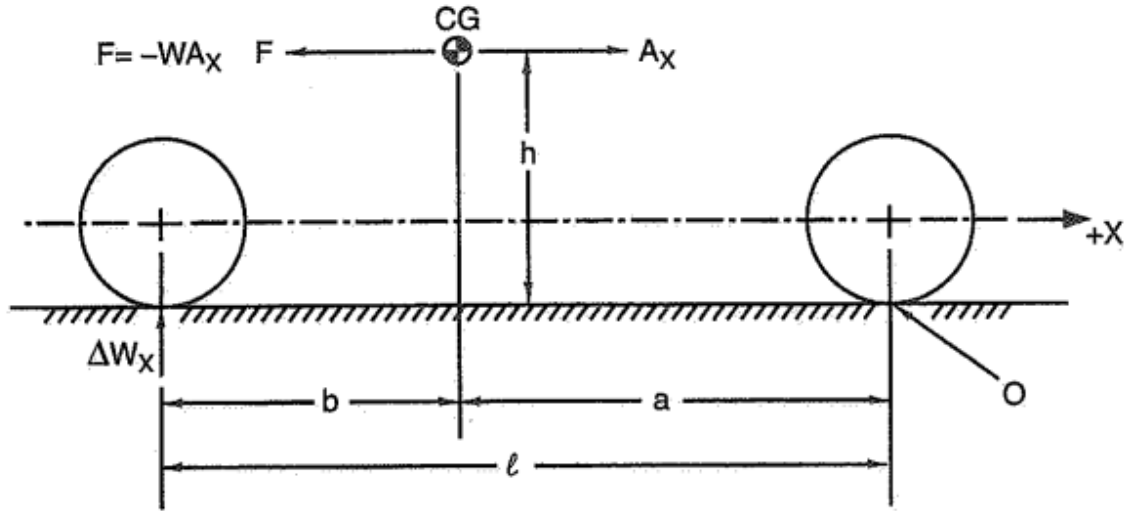


Figure 27 – longitudinal weight transfer during acceleration [17]

$$\Delta F_z = m a_x \frac{h}{l} \quad (8.2)$$

where ΔF_z is the change in tire load; m is the vehicle mass; a_x is the measured longitudinal acceleration; h is the height of the center of mass and l is the wheelbase. This change in tire load will be also present on the front axle as well, but in the opposite direction. The front and rear wheel loads then will be:

$$F_{z,front} = \frac{1}{2} \left(F_{z,front,static} - m a_x \frac{h}{l} \right) \quad (8.3)$$

$$F_{z,rear} = \frac{1}{2} \left(F_{z,rear,static} + m a_x \frac{h}{l} \right) \quad (8.4)$$

where $F_{z, rear, static}$ and $F_{z, front, static}$, describe the static loads on the wheels. Equations are halved, because we are examining the coefficient of friction of one tire instead of the whole axle.

If we now look at data from acceleration of FS.14 without using hybrid power (only rear wheel drive), we can see that the peak longitudinal acceleration achieved was 1.42 g.

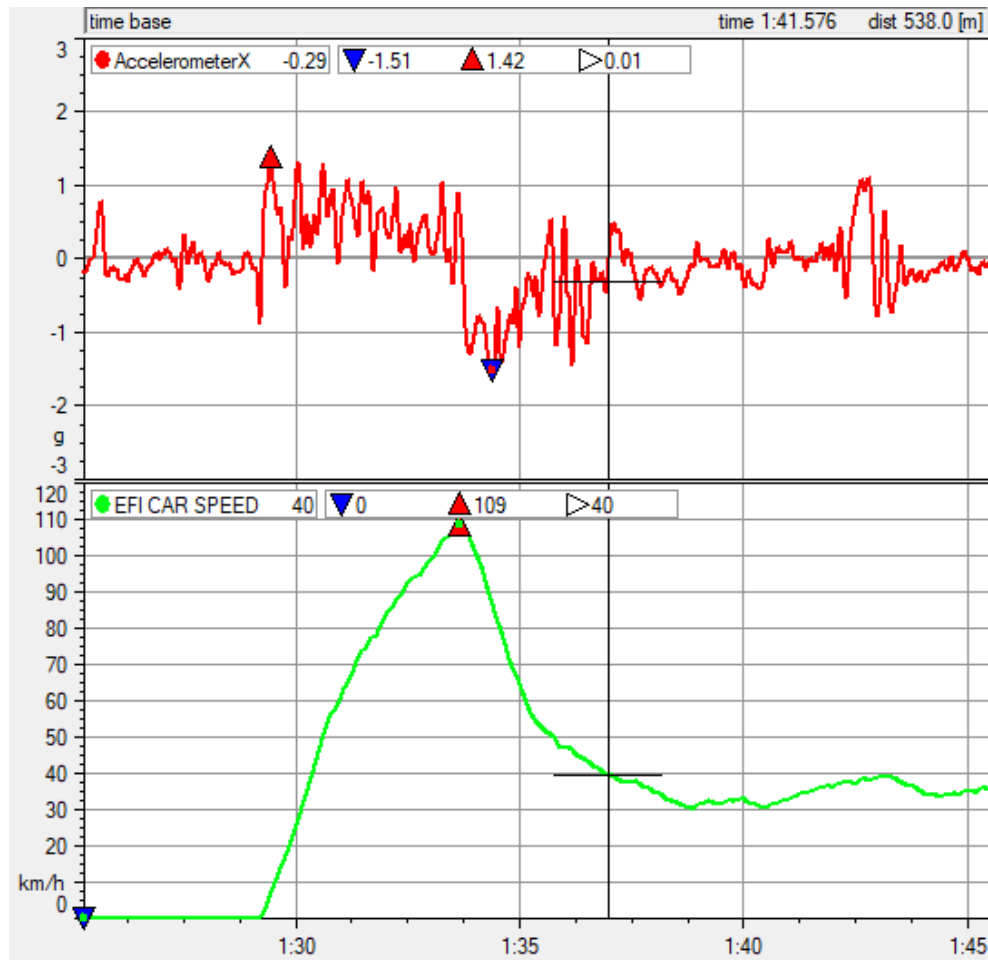


Figure 28 - acceleration and speed data from Acceleration event on FS.14 without hybrid power (x axis is time)

If we then plug in the parameters of the vehicle, we get:

$$F_{z,rear} = \frac{1}{2} \left(1353.8 + 276 \cdot 13.9 \cdot \frac{0.27}{1.53} \right) = 1015.4 \text{ N}$$

(8.5)

And after plugging the result into the equation(8.5)we get the resulting coefficient of friction:

$$f_x = \frac{m \cdot a_x}{2 \cdot F_{z,rear}} = \frac{276 \cdot 13.9}{2 \cdot 1015.4} = 1.89$$

(8.6)

Since weight transfer at such accelerations is far from negligible, to get closer to realistic results, load sensitivity of the tire should be implemented. Load sensitivity is the dependence of the friction coefficient on the tire load. Essentially, the more the tire is loaded, the less efficient it becomes at generating friction. Longitudinal

load sensitivity is normally smaller than lateral load sensitivity. Since, as mentioned before, no data for the longitudinal dynamics of the tire are available, a conservative assumption must be made, that the longitudinal load sensitivity is the same as the lateral load sensitivity.

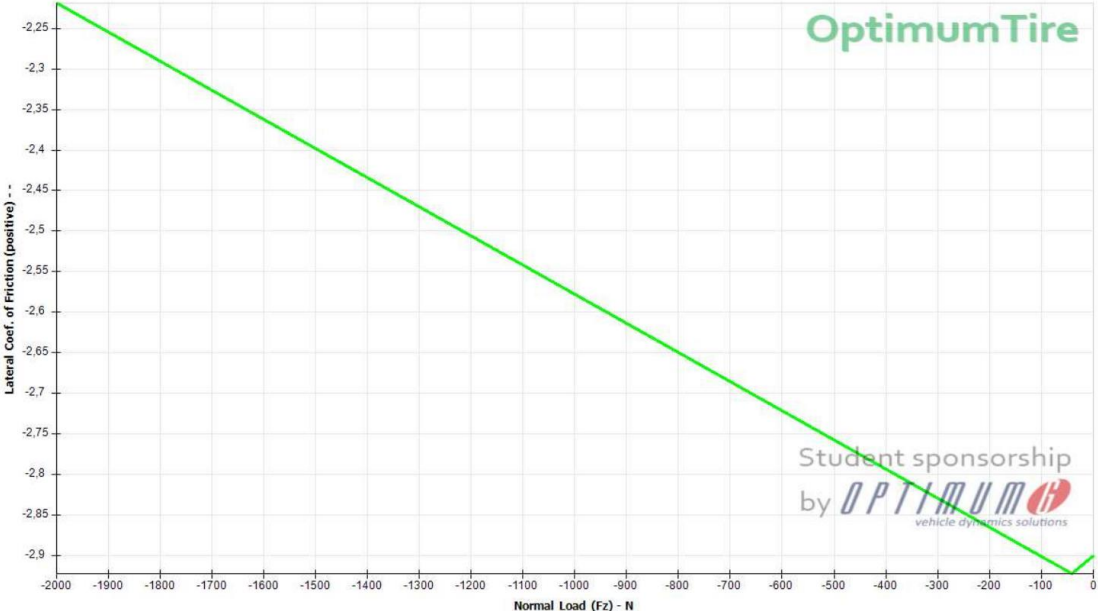


Figure 29 - TTC tire data as analyzed in OptimumTire

Absolute values of the coefficient of friction cannot be simply taken from the test data due to special surface the tires are tested on, however, the load sensitivity slope should be the same as on the track. Therefore, from a friction point known from the test data on the track and the slope from the TTC data we can derive a function of the coefficient of friction dependent on the tire load.

$$f_x = 2.25 - 0.00035 \cdot F_z \tag{8.7}$$

Further, the coefficient of friction is strongly dependent on the slip ratio of the tire. However, with no tire data to use for this calculation, an assumption that the best measured acceleration was within the optimal slip ratio of the tire must be made. Any other projection would be an optimistic guess, since in practice, a better acceleration than shown in Figure 28Figure 1 hasn't been recorded.

Additionally, since we need to calculate the grip potential over a range of different speeds, load transfer from aerodynamic drag must be added to the effect

of weight transfer due to acceleration. The total loads on the front and rear axle will then be >

$$F_{z,front} = F_{z,front,static} - ma_x \frac{h}{l} - F_{x,drag} \frac{d-h}{l} \tag{8.8}$$

$$F_{z,rear} = F_{z,rear,static} + ma_x \frac{h}{l} + F_{x,drag} \frac{d-h}{l} \tag{8.9}$$

where $F_{x,drag}$ is the resulting aerodynamic drag and d is the height of the center of pressure in the YZ plane.

From this, the longitudinal acceleration potential can be easily calculated using the equations derived above. To include the added traction from the front tires the maximal traction forces from both axles will be summed and will provide the total driving force.

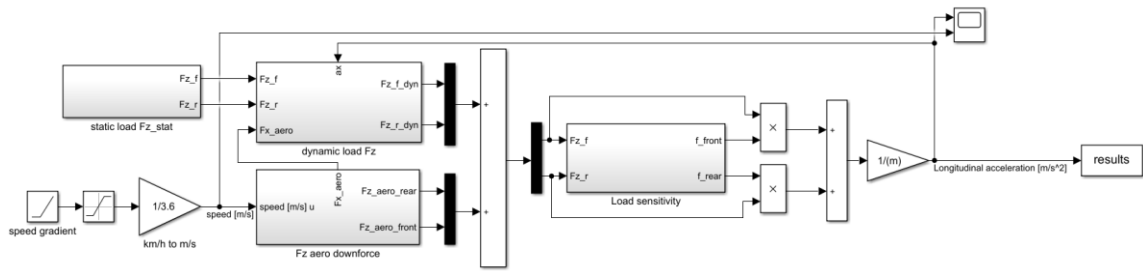


Figure 30 - Simulink simulation of maximal long. acceleration depending on changing speed

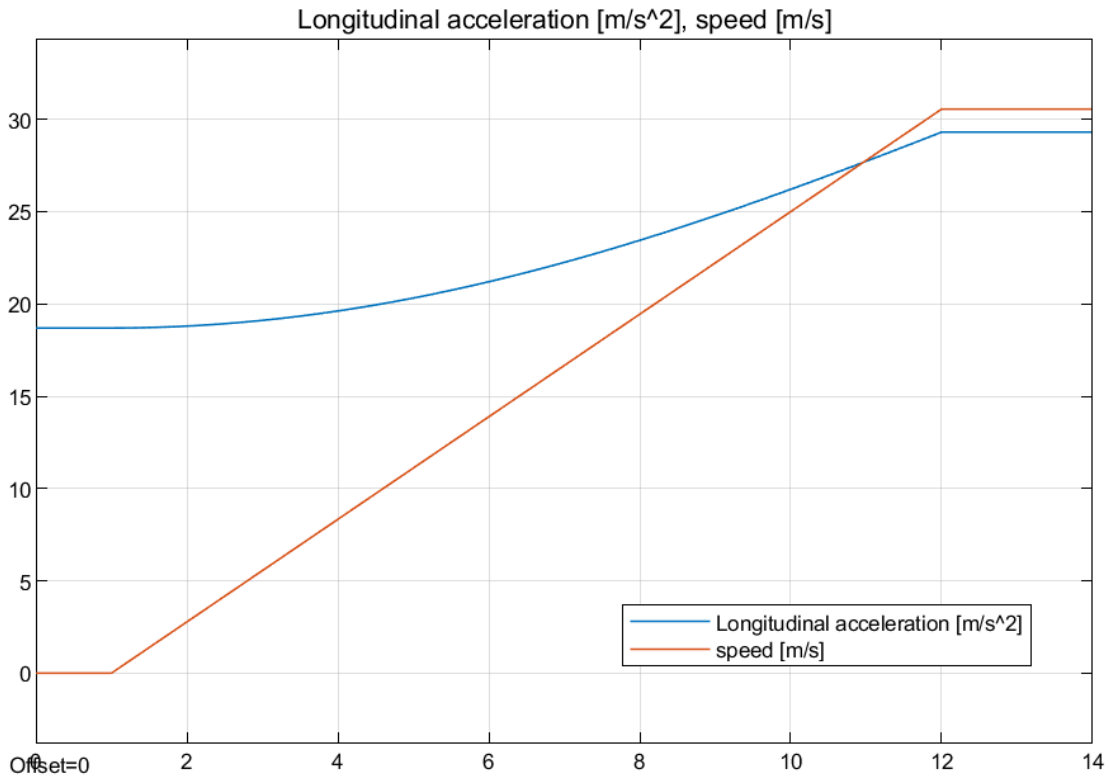


Figure 31 - simulation of maximal longitudinal acceleration with aerodynamic forces

This will provide the longitudinal part of the g-g-v diagram needed for the estimation of the initial velocity profile.

8.2. Longitudinal dynamics

Further, since there is an additional and separate powertrain providing driving force to the vehicle, the equation for resulting force will have an additional term, the drive of the electric motors F_E .

$$F_{net} = F_D + F_E - F_B - F_R - F_C - F_A - F_I \quad (8.10)$$

The force from the electric motors will be controlled by an algorithm (described in the following chapters), which takes as inputs the throttle pedal position, the brake pedal position, the current vehicle speed v and the state of charge of the battery SOC . The real control algorithm on the vehicle will be more complicated.

$$F_E = F_E(throttle, brake, v, SOC) \quad (8.11)$$

As described in chapter 7.2, the model of a driver regulates the throttle input to match the initial velocity profile. Since the initial velocity profile now takes into account also the grip available on the front axle, without any modification of this regulation, the simulation would use this added grip regardless of the axle on which it is available, and in the regions, where the rear axle is grip limited, the total acceleration would result in too optimistic accelerations. For this reason, an additional limitation for the driving force of the ICE, F_D , must be introduced to the simulation. Based on a g-g-v diagram derived for the rear wheel drive only, the limiting traction for the rear axle can be determined. Such limitation can be achieved by approximating the g-g diagram at the given speed to have an elliptical shape.

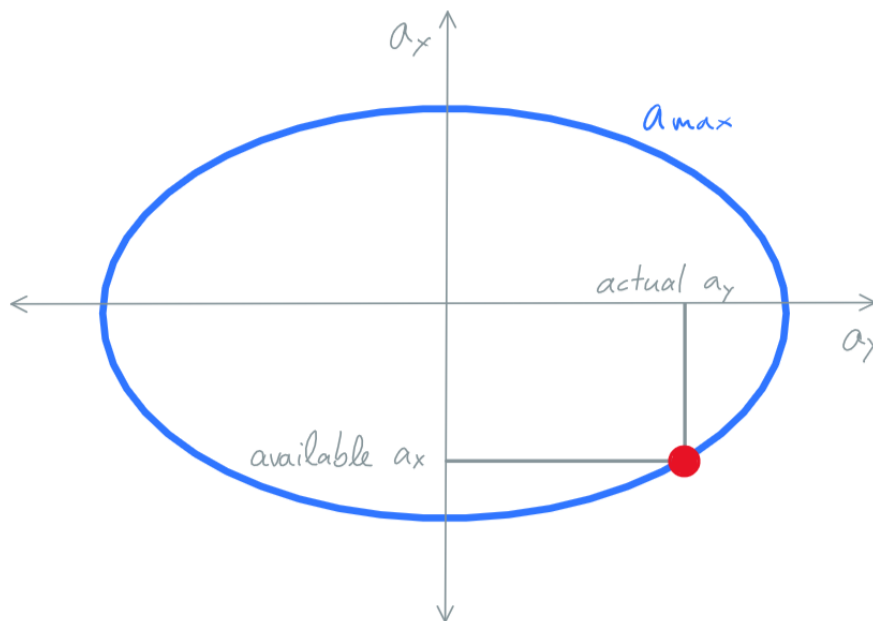


Figure 32 - illustration of the rear axle limitation

Such limitation then can be realized by the following Simulink diagram.

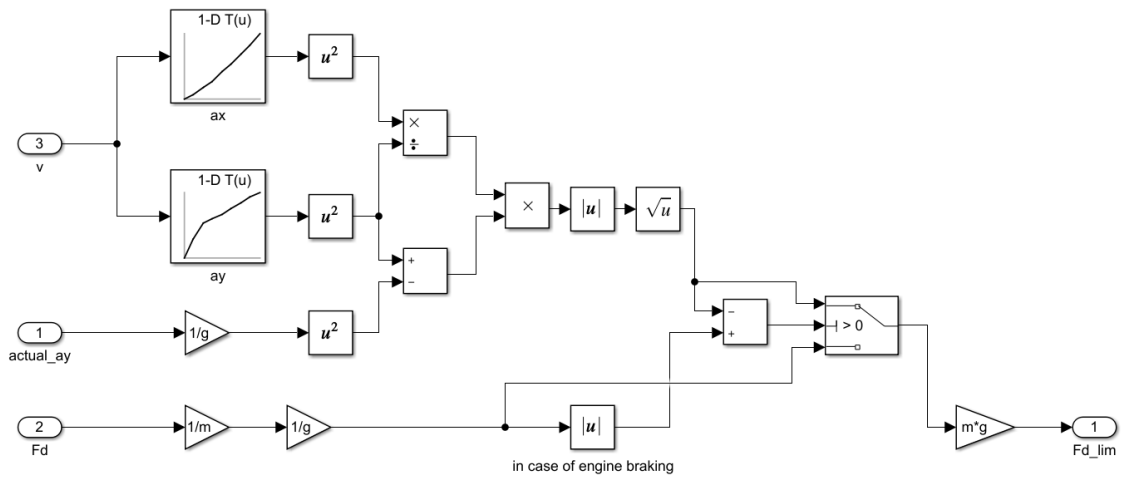


Figure 33 - realization of grip limitation of the rear axle in Matlab Simulink

Since the new model which includes the hybrid powertrain also has additional parts, the inertial resistance of those parts, namely the electric motors and the planetary gearboxes, must be taken into account in the calculation of the reduced moment of inertia of the whole vehicle.

$$J_{red,i_g} = 4 \cdot J_W + i_{diff}^2 \cdot J_{Dr} + i_{g(i)}^2 \cdot i_{diff}^2 \cdot (J_E + J_C + J_G) + 2 \cdot i_{PG}^2 \cdot J_{EM} + 2 \cdot J_{PG} \quad (8.12)$$

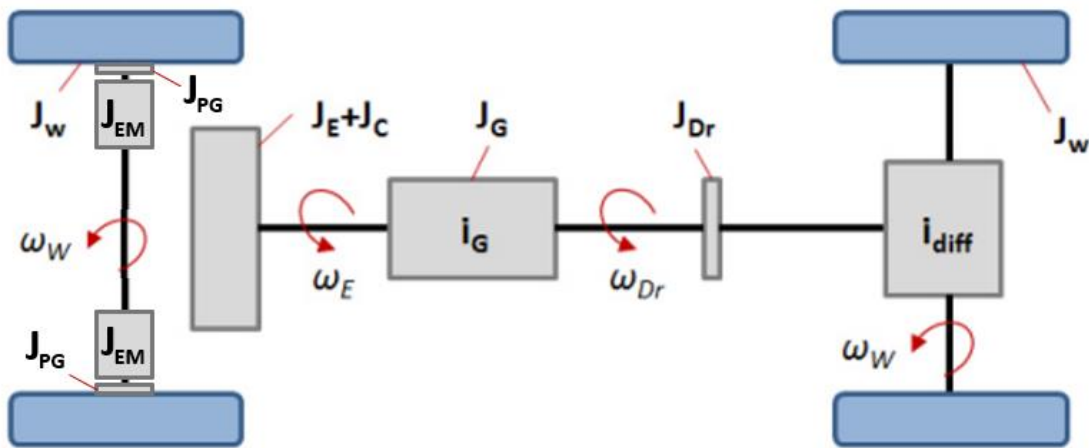


Figure 34 - schematic model of the powertrain

8.3. The electric powertrain model

The FS.14 is going to be using 2 synchronous motors with permanent magnets, each integrated in one of the front wheels and fitted with a planetary gearbox.

For the modelling of the electric powertrain, there are multiple approaches that could be used. There are complex approaches, like for example an Ansys model, but those increase the simulation time considerably and such models wouldn't be suitable either for optimization tasks or real-time control. On the other hand, an empirical PMSM (permanent magnet synchronous motor) model could be used. In the PMSM model, the electric dynamics can be expressed as follows [22].

$$\frac{di_{sd}}{dt} = \frac{u_{sd}}{L_d} + \frac{L_q}{L_d} p \omega_m i_{sq} - \frac{R_s}{L_d} i_{sd} \quad (8.13)$$

$$\frac{di_{sq}}{dt} = \frac{u_{sq}}{L_q} + \frac{L_d}{L_q} p \omega_m i_{sd} - \frac{R_s}{L_q} i_{sq} - \frac{\psi_{pm}}{L_q} p \omega_m \quad (8.14)$$

$$\frac{d\varphi_m}{dt} = \omega_m \quad (8.15)$$

where u_{sd} and u_{sq} are the stator voltages in the d-axle and q-axle, respectively; i_{sd} and i_{sq} are the stator currents in the d-axle and q-axle, respectively; R_s is the stator resistance; L_d and L_q are the equivalent inductances in the d-axle and q-axle, respectively; ψ_{pm} is the electromotive force; p is the number of pole pairs and ω_m is the mechanical spin of the rotor.

The output torque of the PMSM model can be described as follows.

$$T_e = \frac{3}{2} p [\psi_{pm} i_{sq} + (L_d - L_q) i_{sd} i_{sq}] \quad (8.16)$$

This model, however, adds unnecessary complexity, while the only values used for the simulation are the available torque of the motors and the efficiency at given RPM and torque. Those values are supplied by the manufacturer and can be measured on a test bench in case of a post-production design change. For this reason, I chose to use two lookup tables, one for the available torque and one for the efficiency.

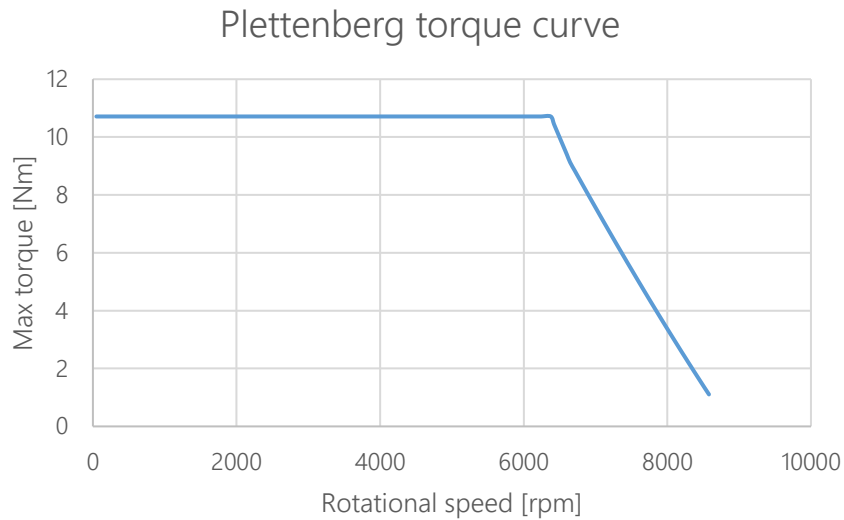


Figure 35 - Torque curve of the used electric motor [23]

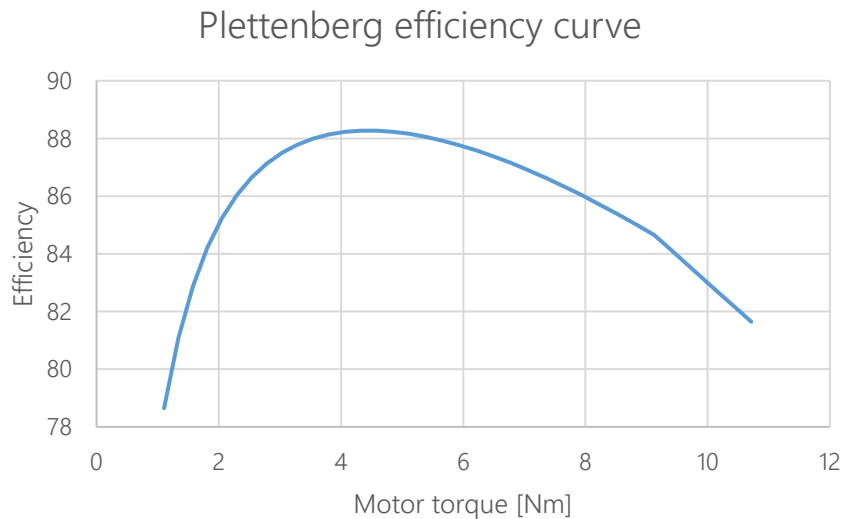


Figure 36 - Efficiency curve of the used electric motor [23]

8.4. Energy consumption

Apart from fuel consumption implemented in the original simulation an additional model of the battery for the analysis of consumption of electrical energy has to be created. The parameters of a battery change with the current going through it, with its state of charge, number of cycles and with the temperature of the battery cells. The battery of FS.14 and its cooling are designed for excessive overloading of the battery cells above the datasheet specification. This, however, hasn't been tested yet and it is a subject to the long-term design plan. For now, in

this simulation and on the track, the battery usage will stay within the limits specified by the manufacturer [24]. This allows for an assumption, that, if well designed, the cooling of the batteries will be sufficient to keep the batteries within the normal operating temperatures. Therefore, the effect of the temperature will be neglected.

Next, the number of cycles of the battery will affect the maximal capacity of the battery. For this reason, it is recommended to monitor the capacity of the battery and change it for a new one once the capacity decreases considerably and affects the performance of the system. For a simulation of one event, which is the objective of this thesis, it is however, not reasonable to take cycling of the battery into account, since as the simulation will later show, the battery completes only one full discharge per event and around 40 partial cycles (below 10% of full charge) per event. From the datasheet [24], significant capacity decrease (10%) happens after more than 300 full charge cycles, which means we can safely neglect this parameter for the optimization.

Lastly, the effect of current going through the battery and the state of charge will affect the voltage of the battery. This, together with the internal resistance of the cells, will be taken into account for the calculation of the waste heat generated in the battery pack. Data from the datasheet will be used in a lookup table to provide this information.

ANR26650M1B Discharge Voltage Profiles
25°C Ambient Temperature In Open Air

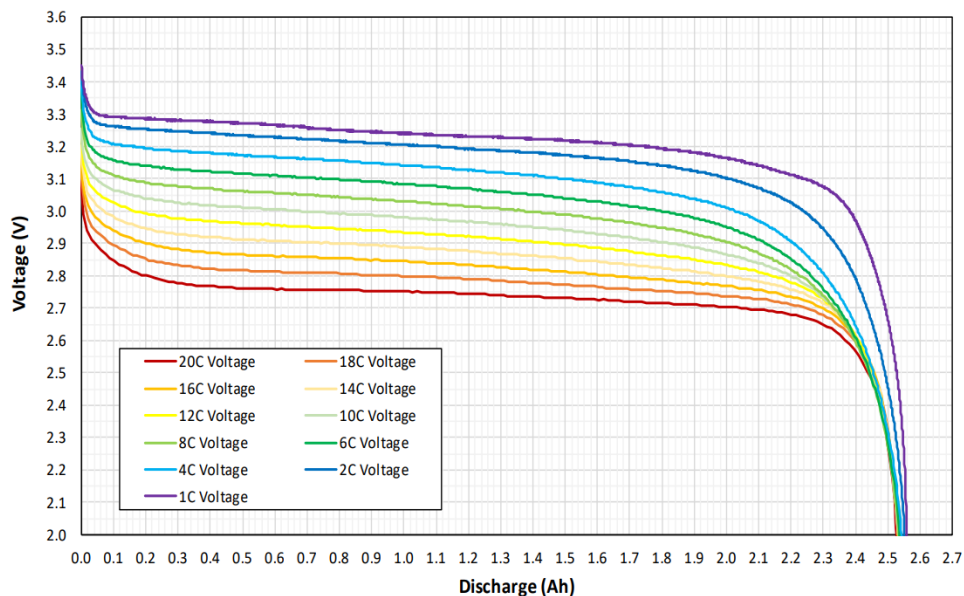


Figure 37 - battery cell discharge voltage profiles [24]

9. CONTROL ALGORITHMS

The control algorithm in this work is aimed at determining the total driving (or braking) torque applied to the front axle to serve as an accelerating (or braking) force for the lap time simulation. The control algorithm for the electric motors will differ when used on the real vehicle and when used in the simulation. However, there will be some overlap, so firstly I will define the common requirements and then the requirements that only apply to the real vehicle.

The common requirements for the control algorithms are:

- the battery must be protected from overcharging or overdrawing over or below a specified voltage (defined as state of charge, SOC),
- the battery must be protected from drawing (or charging) too much current,
- the driving torque should be predictable for the driver (initial drive torque demand),
- the motors should save energy at the end of straights
- the motors should recuperate when coasting,
- recuperation should increase during braking.

The real system on the vehicle will be more complex than in the simulation and therefore the control algorithm will have additional requirements:

- the front wheels must match the speed of the rear wheels – **traction control**,
- when going around a corner, the front wheels should assist the driver on corner entry and corner exit by increasing the desired yaw moment – **torque vectoring**.

These more complex algorithms are however not necessary for the central topic of this work and a concept of their implementation will only be sketched out briefly in chapters 9.5 and 9.6.

9.1. Initial drive torque demand

Multiple strategies of mapping the throttle pedal position to the torque demand of the electric motors could be conceived. It is useful to have different torque demand maps for different choice of tires, different weather conditions or even for different disciplines or drivers. However, an important fact to keep in mind is that the main driving force comes from the ICE on the rear axle of the vehicle. The torque demand provided by the ICE will be controlled by an ETC (electronic throttle control) in the future, thus such mapping strategy will already be implemented there. The main goal of the motors on the front axle is to assist the driver on corner exits and provide additional acceleration on the straights. If the torque on the front axle during driving on the limit would differ from what the driver would expect it could greatly affect the performance and compromise safety. For example, if the cars balance was tuned to be slightly oversteering, then an overly aggressive torque demand map for the electric motors could cause the front tires to exceed their traction limits earlier than the rear tires and make the car understeer.

For that reason, I chose a safe and conservative strategy of static power split between the axles. This split will be defined by a constant parameter, rearward torque bias R_T , which will assume values between 0 and 1. The resulting driving torque demand M_{drive} will be determined by the following equation.

$$M_{drive} = \frac{M_{ICE} \cdot i_g \cdot i_f \cdot (1 - R_T)}{2 \cdot i_e} \quad (9.1)$$

where M_{ICE} is the torque demand for the ICE, which is a function of the throttle pedal position and RPM; i_g is the gearing ratio of the engaged gear; i_f is the final drive ratio; i_e is the gear ratio of the planetary gearbox on each electric motor and the torque is divided by 2, because for now, we assume equal torque demand for each of the front wheels.

Further, three additional cases must be prevented.

1. ICEs on idle (throttle position 0) generate braking torque.

Such case should not enter the torque demand map in the first place however, a good precaution is detecting such cases and if they occur, setting the torque demand to 0.

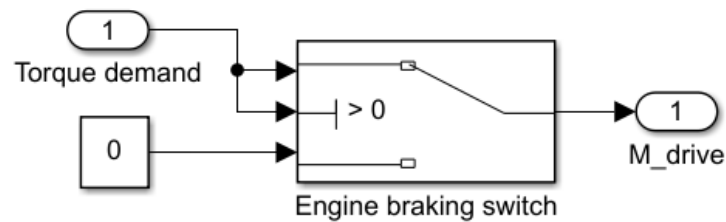


Figure 38 – illustration of filtering out the ICEs braking torque

2. ICEs provide relatively low torque in low RPM.

In a case, when the ICE operates in low RPM, for example a standing start or a very slow corner exit, the front axle might be able to outperform the rear. If that is desirable and a shift in balance of the car is not an issue, the front motors should assist in acceleration. We can assume, that if the driver is pressing the throttle over the full throttle threshold TPS_{full} (for example 90%), the full potential of the front motors should be used. This is realized by a switch block that compares the throttle pedal position TPS to the full throttle threshold. If such event occurs, the driving torque demand M_{drive} is set to the maximal torque available at that speed.

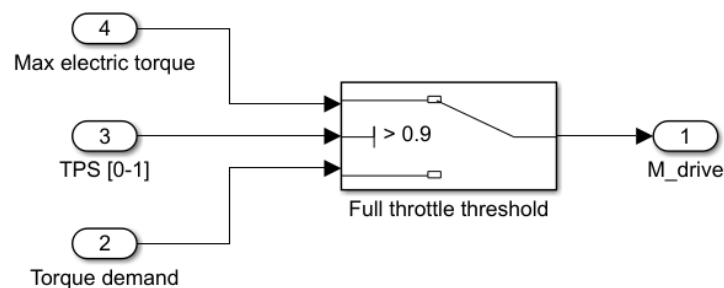


Figure 39 – illustration of detecting the full throttle event

3. Preventing ICEs torque peaks

On the other hand, if the throttle isn't yet fully pressed, but the torque provided by the ICE already exceeds the available torque in the front, the control algorithm shouldn't demand more torque than available. This situation can either happen due to a peak in the ICEs torque curve or in corner exits at higher speeds, where the electric motors are already power limited. The torque demand must be therefore limited by the maximal electric torque available at that speed.

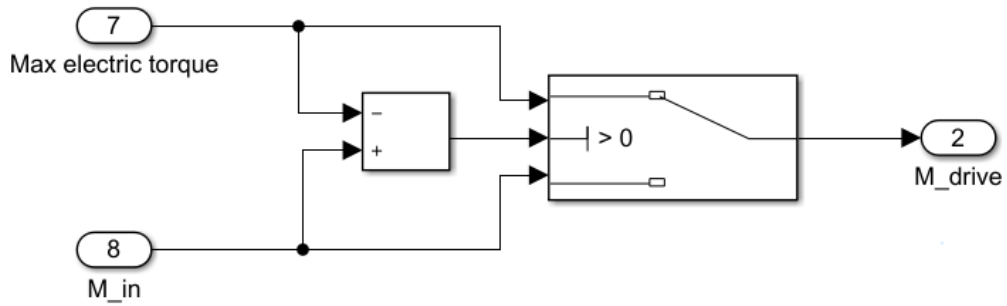


Figure 40 - implementation of maximal available driving torque validation

Finally, an energy saving condition will be introduced. Since the most efficient use of the energy to minimize lap time is at the beginnings of the straights [15], we can assume there is a point at the straight (presumably near the end) at which it is more efficient, when considering the whole length of a race, to disable the electric motors and save energy for other corner exits. Such energy saving strategy can be illustrated on the following drawing.

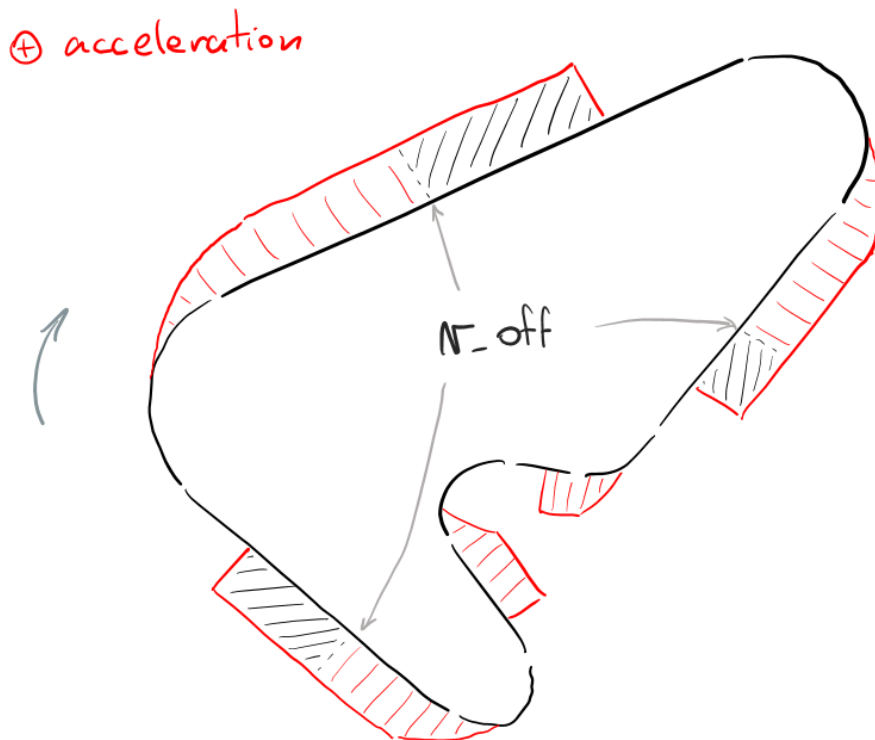


Figure 41 - v_{off} energy saving illustration

The drawing shows a simple racetrack with a clockwise orientation. On the outside of the track a positive energy usage (energy is being used for acceleration) is represented by the red color. Once the vehicle reaches the velocity v_{off} , energy to the electric motors is cut and the area hatched with black lines represents the

saved energy. Such condition can be easily implemented by a switch element and a speed input.

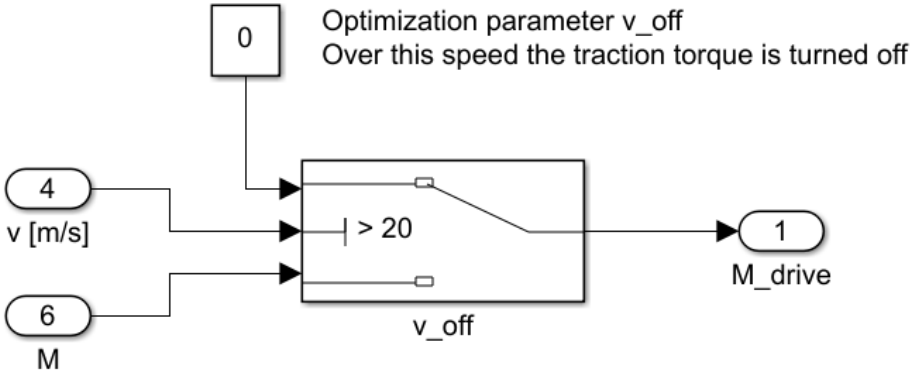


Figure 42 - implementation of v_off energy saving

The following figure shows a full implementation of calculation of the initial torque demand for the electric motors. The resulting torque is in the end multiplied by 2, because this exact Simulink model is used in the simulation, which assumes a single-track model. In the control algorithm of the real vehicle, each motor will have a separate torque demand.

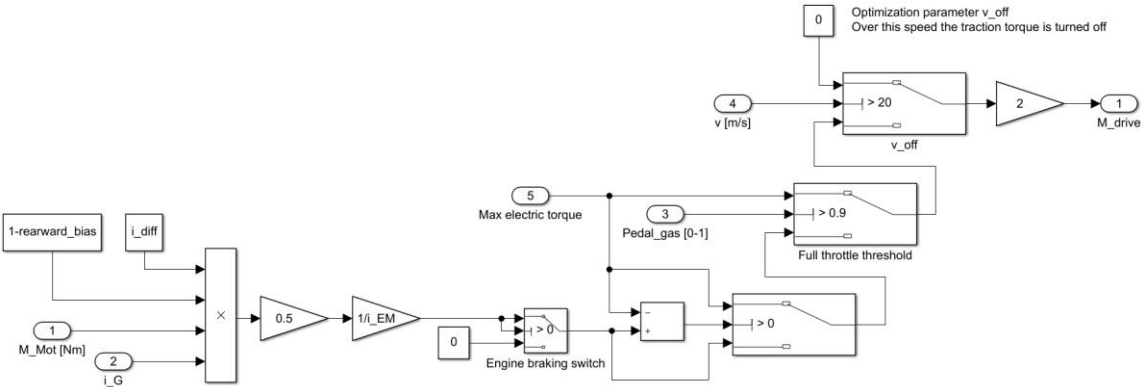


Figure 43 – implementation of driving torque demand in Simulink

9.2. Recuperation control (brake torque demand)

For the design of recuperation control, the following parameters need to be taken into account:

- the utilization of energy from braking,
- the utilization of maximal braking potential,
- the hardware limitations of the brake pedal mechanism
- and the hybrid powertrain concept.

9.2.1. The brake pedal mechanism

Firstly, I'll address the last two points, because they are outside of the scope of this work, but they influence the control design decisions. As per rules T6.1.1 and T6.1.4 a Formula Student monopost must be equipped with a hydraulic brake system that acts on all four wheels and is operated by a single control and no brake-by-wire systems are allowed [1]. Therefore, Formula Student Electric teams that implement recuperation usually construct a 2-phase brake pedal, which in its first phase, before actuating the hydraulic brakes, controls the intensity of regenerative braking. When the pedal is pressed further, the hydraulic brakes are actuated.

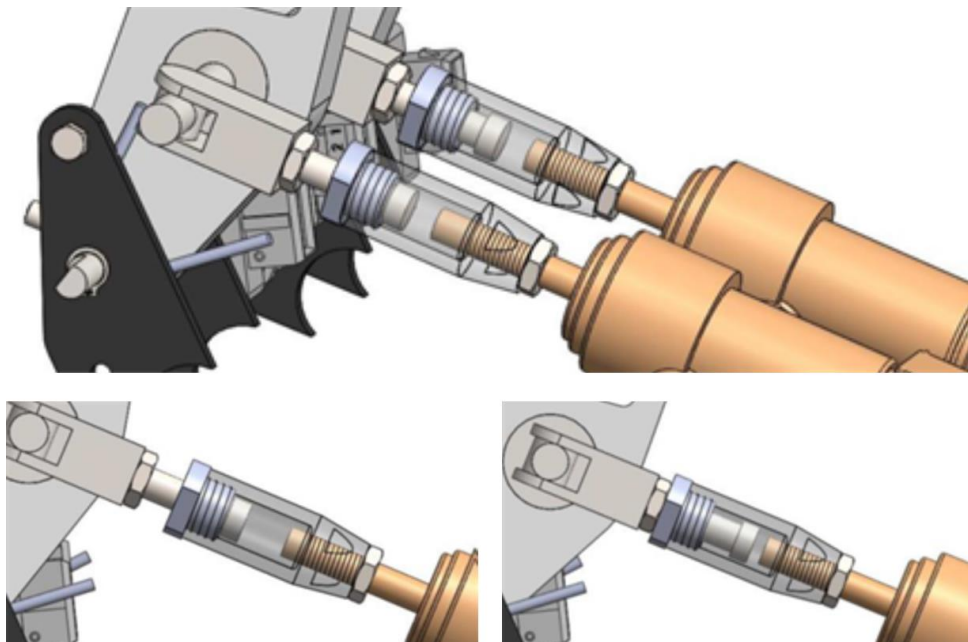


Figure 44 - illustration of a regenerative braking regulator attached to the hydraulic brake piston [25]

Such mechanism, while being very useful for maximizing the regenerated energy, has not yet been designed for the FS.14, so the only other options for recuperation under hydraulic braking is to take the inputs from the brake pressure sensors.

9.2.2. The hybrid powertrain concept

Formula Student Electric vehicles which employ a four-wheel drive in their concepts, have a significant advantage over a rear-wheel drive electric cars or, as in our case, a front-wheel hybrid powertrain. In a 4WD architecture the braking torque can be split between front and rear in a way that maximizes the recovered energy while keeping the optimal brake balance for maximizing the braking effect. Vehicles with an electric powertrain only on one of the axles either compromise the utilization of energy from braking [26] or shift their brake balance towards the driven axle and compromise the maximum braking potential. This, together with the limitation of the brake pedal mechanism limits us to recuperation proportional to the brake pressure supplied by the brake cylinders.

9.2.3. The brake balance and recuperation gain

As partly examined in the previous chapter, the vehicle concept of FS.14 is not optimal for maximizing both the braking force or the recuperation of energy from braking. To fully understand this effect a brief examination of the dynamics of braking and the braking mechanism is necessary.

In a vehicle with a dual master cylinder set-up, the pedal force is usually split between the two master cylinders with an adjustable balance bar. The maximal braking force is achieved when all four tires are brought to the friction peak simultaneously. The optimal brake balance changes with the intensity of deceleration due to weight transfer as described by the following equation [17].

$$N_{f,dynamic} = N_{f,static} + N \left(\frac{a}{g} \right) \left(\frac{h}{l} \right) \quad (9.2)$$

where $N_{f,dynamic}$ is the normal force on front axle during deceleration of a/g ; $N_{f,static}$ is the normal force on front axle with no deceleration but with aerodynamic effects at the speed of interest; a/g is the deceleration of the vehicle in "g" units

(values can range from 5g for high speed with aerodynamic downforce to about 0.1g on ice); h is the height of the vehicle center of mass above ground and l is wheelbase measured in the same units as h .

A similar equation is applicable for the normal force (or load) on the rear axle and it is obvious that a ratio of the loads on the front and rear axle for a given vehicle is a function of deceleration a . The achieved deceleration is different for each corner (because of different speeds), for different application of the force to the pedal and different weather conditions. The mechanics of a standard brake system that is well bled (doesn't contain air in the hydraulic system) and has stiff components minimizing the pedal travel provides a near linear application of braking force to each axle with respect to the applied pedal force. Therefore, the brake balance is kept close to constant under all different intensities of pedal force application. An optimal choice of the brake balance setting is therefore a task for the experienced driver and the race engineer.

This means that any additional braking torque only supplied to the front axle that is not strictly proportional to the brake force applied by the master cylinder will change the brake balance and thus compromise the optimal brake balance. This leads to three possible strategies of braking energy recuperation, either of which will compromise the overall lap time, but might compensate for it with the additional energy provided to the system. The exact setting of some of these strategies will be recommended by the results of the optimization task, but ultimately will be left to be tuned by the driver or the race engineer on track.

1. Proportional braking with respect to the brake pressure in the system

As already examined, this compromises the maximal recuperated energy. However, there is an additional limiting factor which is the charging limit of the battery. At higher speeds the front motors won't be able to proportionally match the braking force of the hydraulic system and as such, this seems as the least effective option. The following drawing illustrates the amount of energy generated during braking initiated by the brake pedal (not drawn to scale).

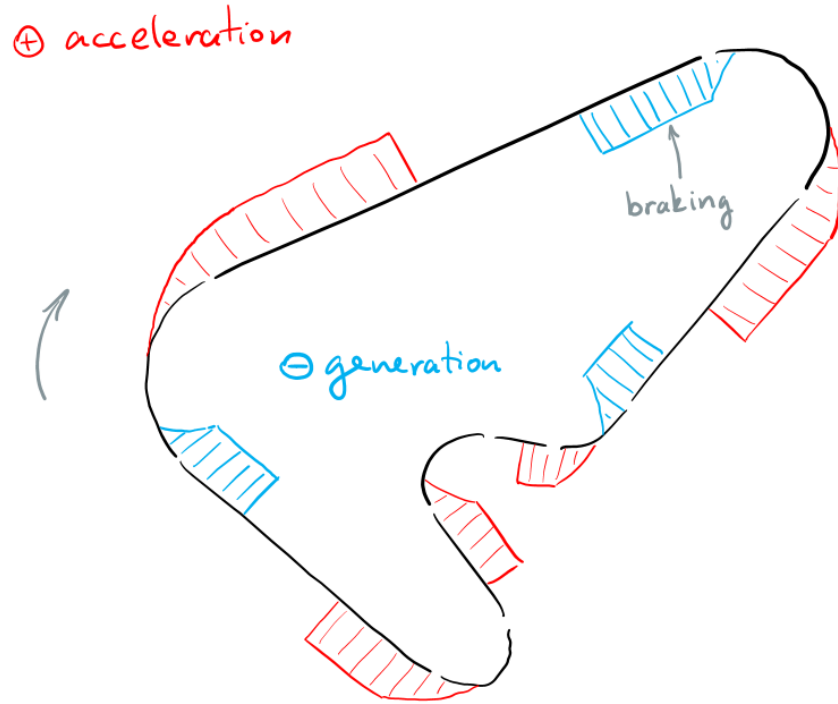


Figure 45 - illustration of energy generation during braking

This strategy can be realized, most simply, by introducing a constant gain to the signal from the front brake pressure sensor BP .

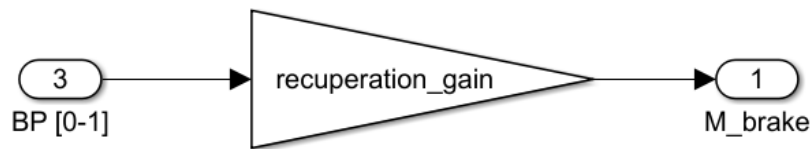


Figure 46 - illustration of an implementation of proportional recuperation

2. Constant recuperation during acceleration over a specified threshold speed

It is conceivable, that sacrificing some amount of acceleration close to the end of a straight, in a region where the driving torque from the ICE dominates the acceleration force and the vehicle is not traction limited, could be more efficiently utilized in the corner exits, where the additional friction from the front axle is the most useful. The following drawing illustrates the two parameters defining this strategy (the parameters will be subject to optimization in chapter 10).

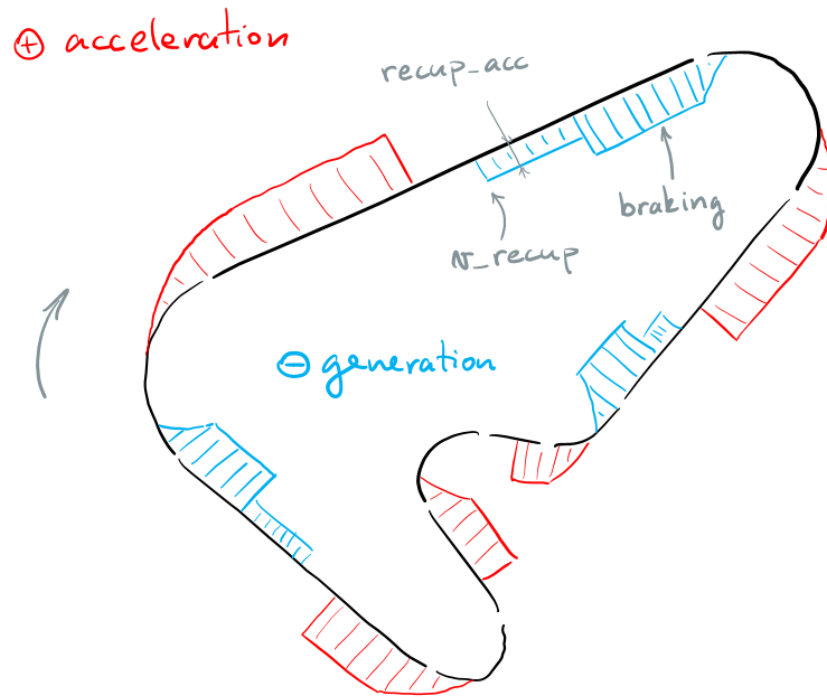


Figure 47 - illustration of energy generation during acceleration by the ICE

The blue areas in the "negative" region of the diagram represents the energy generated by the electric motors in a braking mode. Before the driver initiates braking, the front motors start generating energy once the vehicle reaches speed **v_recup**. The amount of braking torque will be specified by the **recup_acc** parameter (on the illustration represented as power).

This strategy can be realized by a switch element, a constant specifying the acceleration recuperation and a signal from the vehicle speed channel **v**.

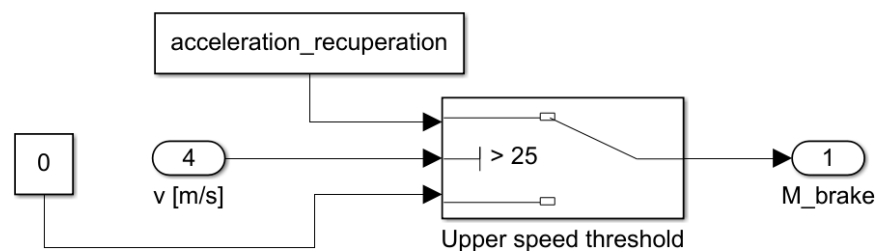


Figure 48 – illustration of the implementation of acceleration recuperation

3. Constant recuperation during coasting and under a specified throttle threshold

If the vehicle is in a steady state cornering phase and isn't using traction for acceleration, the drive from the rear wheels could be harvested in the front. Loading the tires longitudinally during cornering would compromise the maximal lateral capacity of the tires. Other methods for transferring energy from the engine to the hybrid battery that wouldn't load the tires could be designed (for example waste heat recovery or an alternator, effectively making this series/parallel hybrid). With relatively small braking torques in these states, this effect should not significantly affect the dynamic performance of the vehicle. It is also a reasonable assumption that the less experienced drivers of Formula Student might not be able to exploit the capacity of the tires and would benefit more from corner exits and a quick acceleration. However, for a thorough examination, the simulation model could be adjusted to calculate the difference in cornering ability for each state of the vehicle. For this thesis, I will concentrate on the energetic side of the problem and explore all areas, where energy can be harvested or used. The following drawing illustrates the implementation of this strategy.

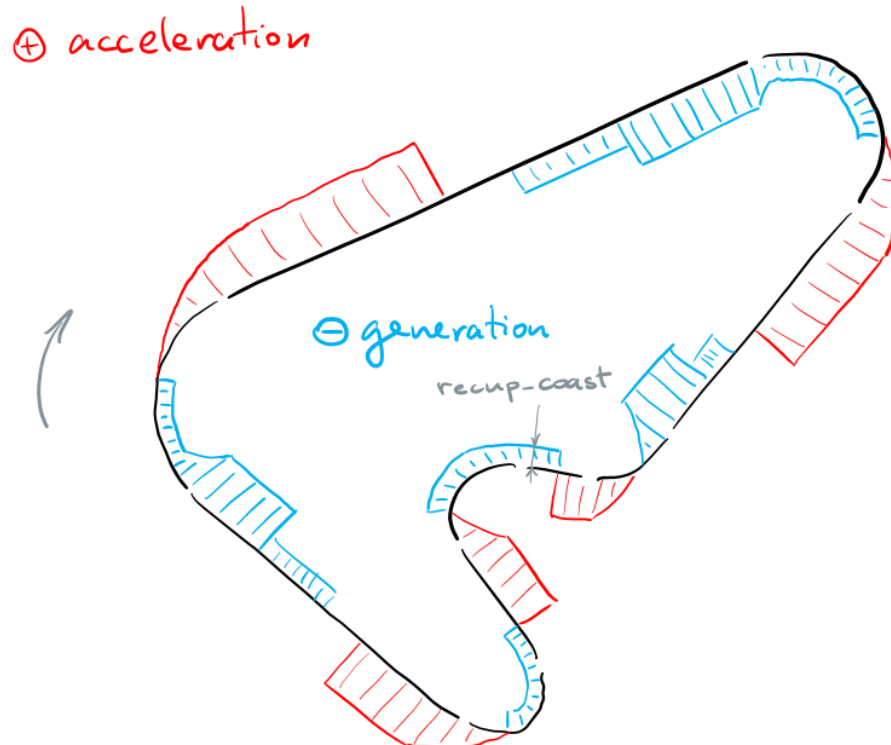


Figure 49 - illustration of energy generation during coasting

A new constant **recup_const** will regulate the amount of braking torque applied during all phases that qualify as coasting (throttle pedal under a certain threshold, close to idle position).

This strategy can be realized by a switch element, a constant specifying the coasting recuperation and a signal from the throttle position sensor *TPS*.

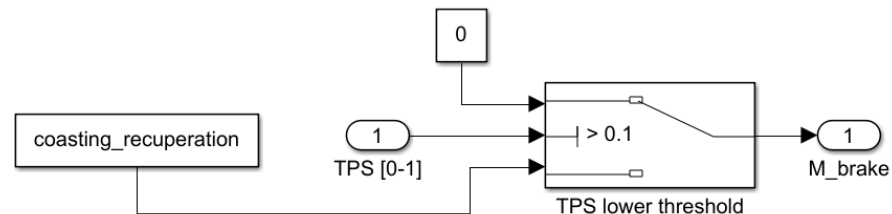


Figure 50 – illustration of implementation of coasting recuperation

Finally, the resulting torque, after multiplying by -1 to match the convention, must be compared to the maximal torque the motors can provide at that speed. If the braking torque exceeds the maximum torque available, the braking torque M_{brake} will be set to the maximum.

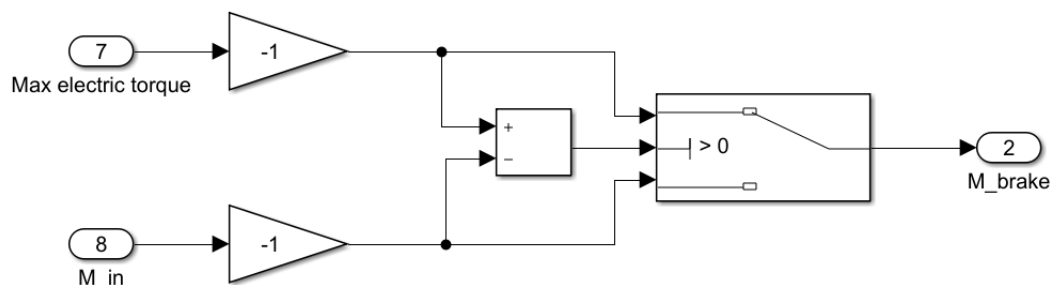


Figure 51 – implementation of maximal available braking torque validation

When we put all of these strategies together, the logic becomes slightly more complicated. To examine the effects of the acceleration and coasting recuperation strategies, it is important for them not to overlap. Therefore, a logic that only allows one of those effects to pass through is implemented. In a case when both conditions are fulfilled, the acceleration recuperation has a priority. The proportional gain from the pedal is always added to the resulting braking torque.

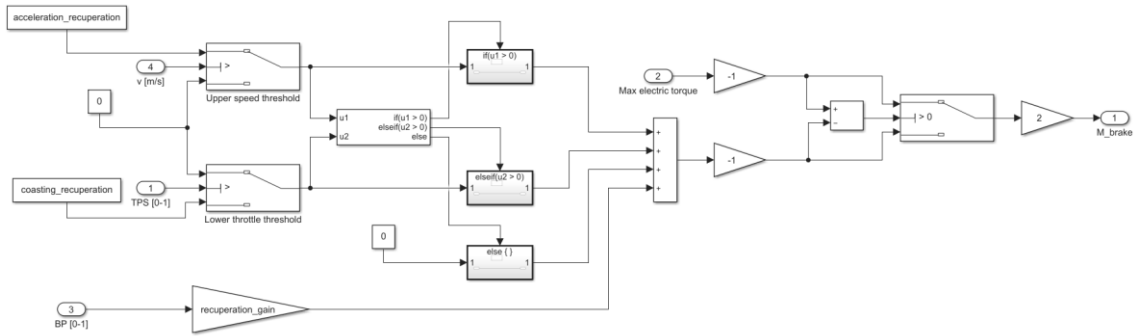


Figure 52 – implementation of braking torque demand in Simulink

Similarly, as in the initial drive torque demand, the resulting torque is multiplied by 2 for the purposes of the simulation. The algorithm for the real vehicle will have separate torque demands for each wheel.

9.3. Overcharging and overdrawing the battery (SOC validation)

To prevent the battery from overcharging during regenerative braking or from overdrawing it during acceleration a simple logic composed of switch elements is implemented. The torque demand M_{in} passes through 2 switches to determine, to assign values to braking torque M_{brake} if the torque demand is negative or to M_{drive} if the torque demand is positive. Default values of both are otherwise zero. That means, only M_{brake} or M_{drive} is assigned a value after this step.

In the next step, the state of charge SOC of the battery is compared to its upper threshold (in the example below 100% of charge) and lower threshold (0% in the example) values. If the SOC is at or below the lower threshold, the drive torque demand M_{drive} doesn't pass through and a default value of 0 is assigned. Similarly, if the SOC is at or over the upper threshold, the braking torque demand M_{brake} doesn't pass through and a default value of 0 is assigned. At the end both resulting values are summed and the output is the resulting torque demand for the electric motors M_e .

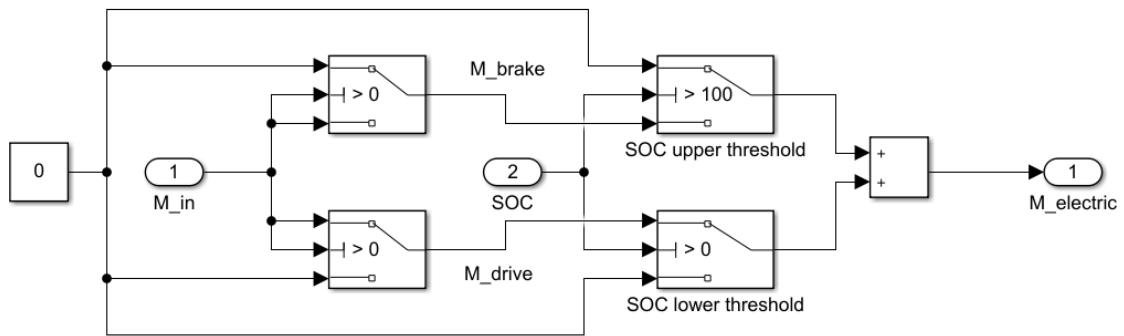


Figure 53 – implementation of SOC validation in Simulink

9.4. Overcurrent protection

Each component in the system has its current (or power) specification which it cannot exceed. The limiting factor in the FS.14 electric powertrain is the battery pack which has a specified peak current values for charging and discharging. As per rule 6.3. in the CV Hybrid Rules Extension the energy storage container must be equipped with an overcurrent protection that trips at or below the maximum specified charge current of the cells [16]. Similarly, the rule 6.5. states that a fuse rated for the maximum specified discharge current of the cells must be implemented [16]. Both rules will be satisfied by the implementation of a battery management system (BMS), however, the control algorithm should prevent either event from happening. For that reason, a similar validation block, as a validation of the SOC, is implemented.

The torque demand M_{in} is also separated into braking torque M_{brake} and driving torque M_{drive} because of different thresholds for charging and discharging. After that, both are converted into power required to fulfil that torque demand (either braking or driving) and compared to their respective thresholds. If the power is out of the bounds defined by the thresholds, the thresholds themselves provide the basis for calculating the new torque demand.

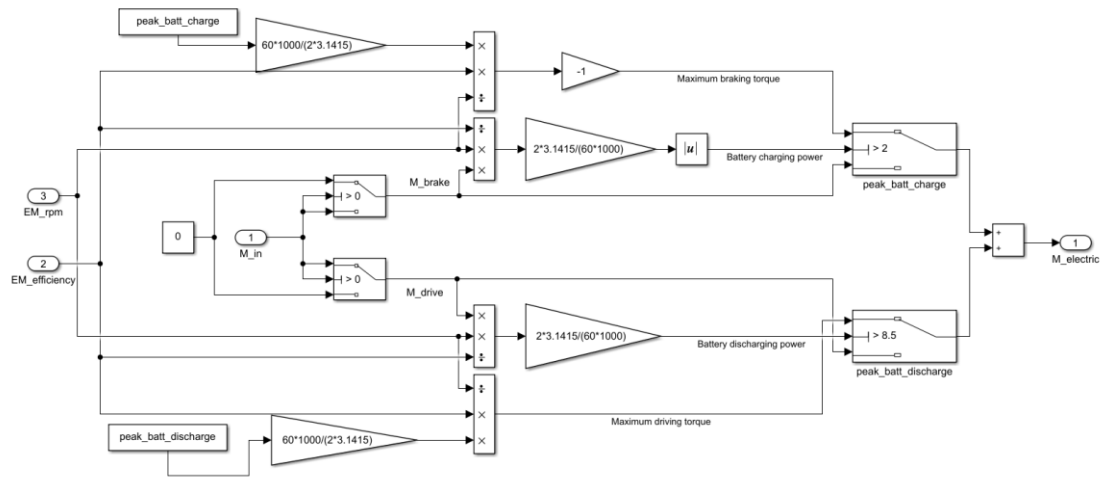


Figure 54 – implementation of overcurrent protection in Simulink

Therefore, if the power needed to supply the driving torque is greater than the peak battery discharge power P_d [kW], a new driving torque is calculated. In that calculation, the efficiency of the motor f and the RPM of the motor n are taken into account.

$$M_{drive} = P_d \frac{60 \cdot 1000 \cdot n \cdot f}{2\pi} \quad (9.3)$$

Similarly, if the power that would result from the braking torque exceeds the peak charging capacity of the battery P_c , a new driving torque is calculated. Braking torque is negative by convention.

$$M_{brake} = -P_c \frac{60 \cdot 1000 \cdot n \cdot f}{2\pi} \quad (9.4)$$

Resulting torques are then summed and the output is the new torque demand for the electric motors M_e .

9.5. Traction control

Traction control is usually achieved by minimizing error between the slip ratio on the driven axle and the target slip ratio for optimal longitudinal traction (from tire data). Slip ratio SR is determined by the following equation [17].

$$SR = \frac{\omega - \omega_0}{\omega_0} \tag{9.5}$$

where ω is the angular velocity of the driven (or braked) wheel and ω_0 is the angular velocity of the free rolling wheel.

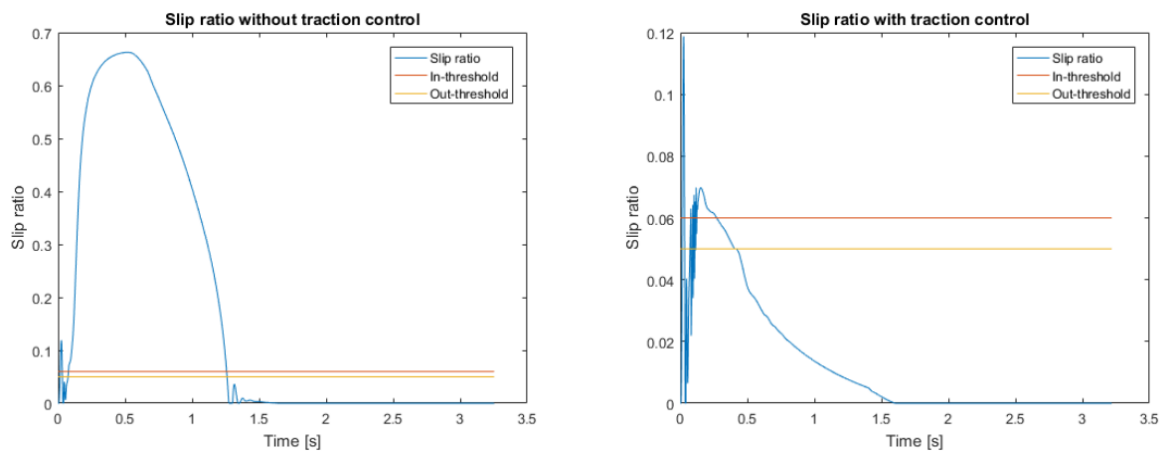


Figure 55 - slip ratio on a driven axle with and without traction control [27]

Reaching the optimal slip ratio maximizes longitudinal friction. This is, however, more complicated in vehicles with no free rolling wheels. Since in the concept of FS.14 all wheels are driven, the reference for traction control must be found elsewhere. For such applications, data from high frequency GPS combined with corrections from inertial sensors are sometimes used.

For our application, it is at the very least necessary to ensure, that if the front wheels lose traction, they won't reach run-away RPM. Since the motors are torque controlled, it is conceivable that on a low traction surface or due to a damaged tire, a torque demand might cause the wheel to spin with speeds much higher (or lower during braking) than the rear wheels. Therefore, a form of traction control similar to the example above could be introduced, but it would measure the slip ratio between two driven axles and have much wider thresholds. Rather than maximizing longitudinal grip, this basic algorithm should be a safety feature before introducing a more complex traction control in the later stage of development.

9.6. Torque vectoring

Torque vectoring is an effective method of controlling yaw rate with the to yaw moment given to a vehicle. Torque vectoring systems can effectively maintain stability and increase response through a large range of vehicle operations [28].

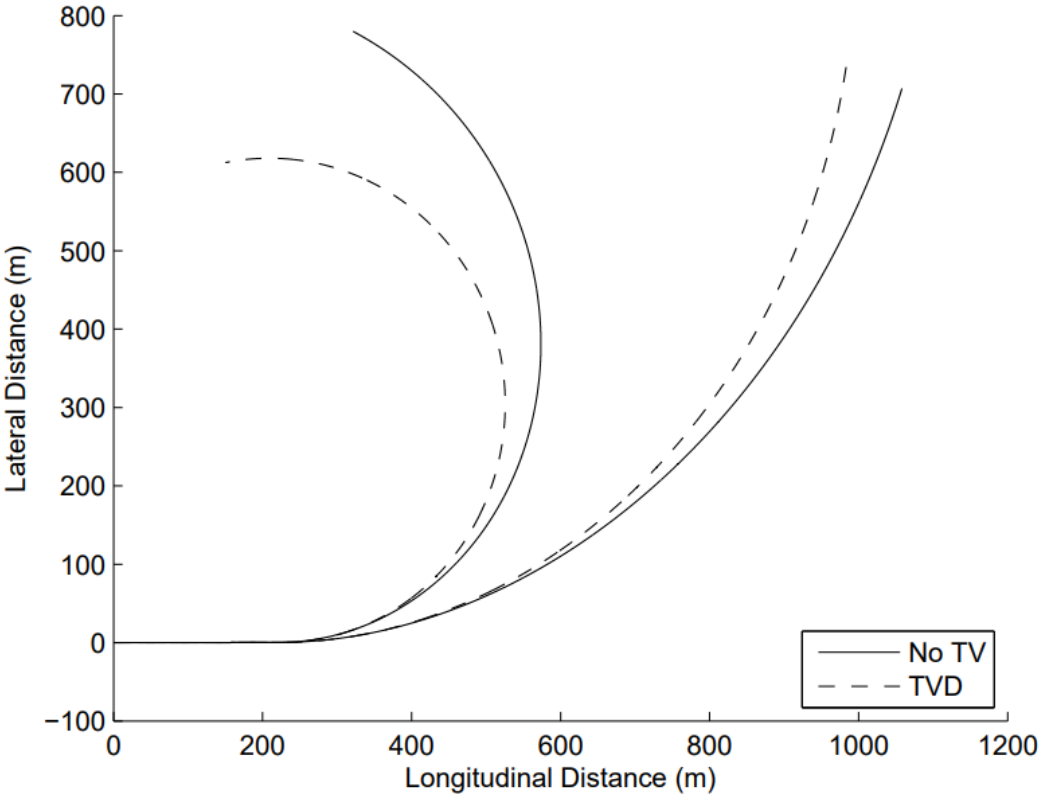


Figure 56 – cornering with and without torque vectoring. [28]

Various methods of yaw moment control are conceivable. It can be realized by differentials, brakes or electric motors or active rear wheel steering. In the concept of FS.14 the front motors can be utilized in this way to improve lap time in corner entry and exit.

Torque vectoring (TV) yaw rate control is achieved through biasing torque at the wheels in order to control the yaw rate more effectively than by turning the front wheels alone. The most used example for explaining torque vectoring is the yaw rate control of a tank. The tracks of a tank cannot be turned like wheels on a car to produce a desired yaw moment necessary for turning, therefore, a differential torque is applied to the left and right tracks [28].

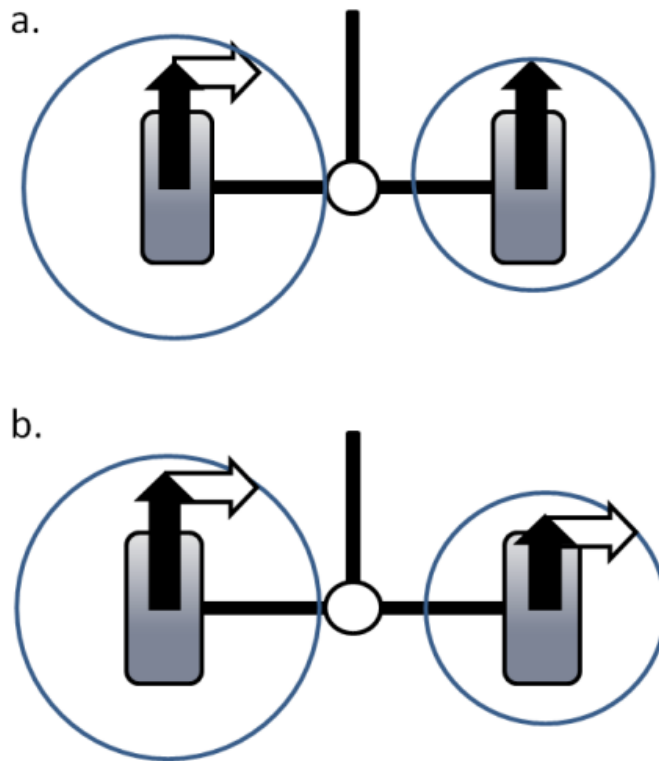


Figure 57 - torque vectoring (b.) improves traction and cornering by distributing torque more effectively [28]

TV control is usually split into an upper and lower controller. The upper controller determines the desirable yaw moment to best assist the driver based on the steering wheel and pedal inputs. The desired yaw moment can be calculated from a single-track model of the vehicle and real time values from the sensors. The lower controller acts upon this to decrease the difference of the measured yaw rate to the desired yaw rate by applying yaw moment, in our case, by a differential torque on the front wheels. For this a kinematic model and the current positions of the steering geometry must be taken employed.

9.7. Summary

The control algorithms described above with the exception of torque vectoring and traction control are grouped to thematic blocks (same as the chapters here) and together provide a complete algorithm for determining the resulting torque on the front axle based on the state of the vehicle (state of charge of the battery, speed of the vehicle, torque provided by the ICE and the engaged gear) and the driver's inputs (position of the throttle pedal and the brake pressure). The next page is dedicated to a display of the full implementation of the electric torque control algorithm.

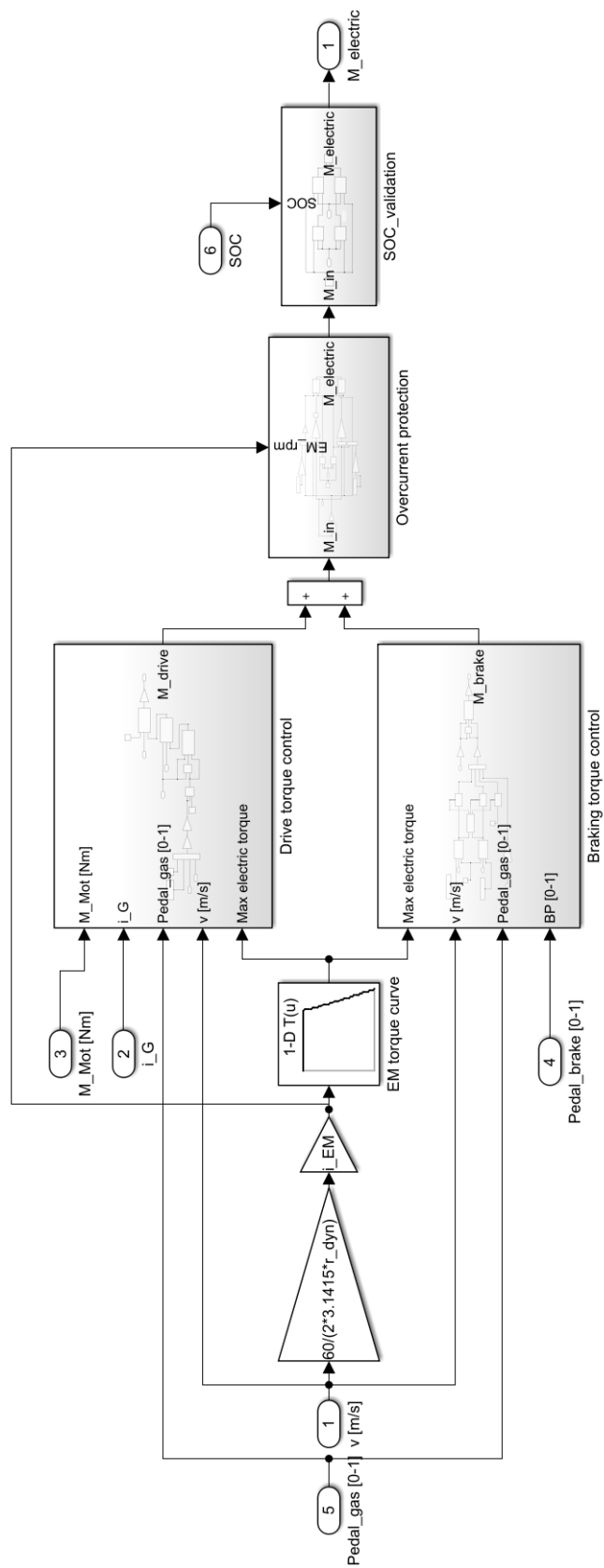


Figure 58 - the full implementation of the electric torque control algorithm

10. OPTIMIZATION

When comparing the effect of the hybrid system (taking into account also the 16 kg of added weight), the car is quicker in most disciplines, but loses a lot of time in Endurance.

Table 8 - overview of times per discipline before optimization

Discipline	Maximum points	FS.13 (no hybrid)	FS.14 (hybrid)
Endurance	325	1352.8 s	1364.3 s
Efficiency	100	3.03 l	3.00 l
Autocross	100	67.6 s	66.9 s
Skidpad	75	5.12 s	5.16 s
Acceleration	75	3.62 s	3.38 s

After the initial simulation of Endurance discipline, it is obvious that the energy runs out quite early, in lap 4, even with the basic recuperation during braking.

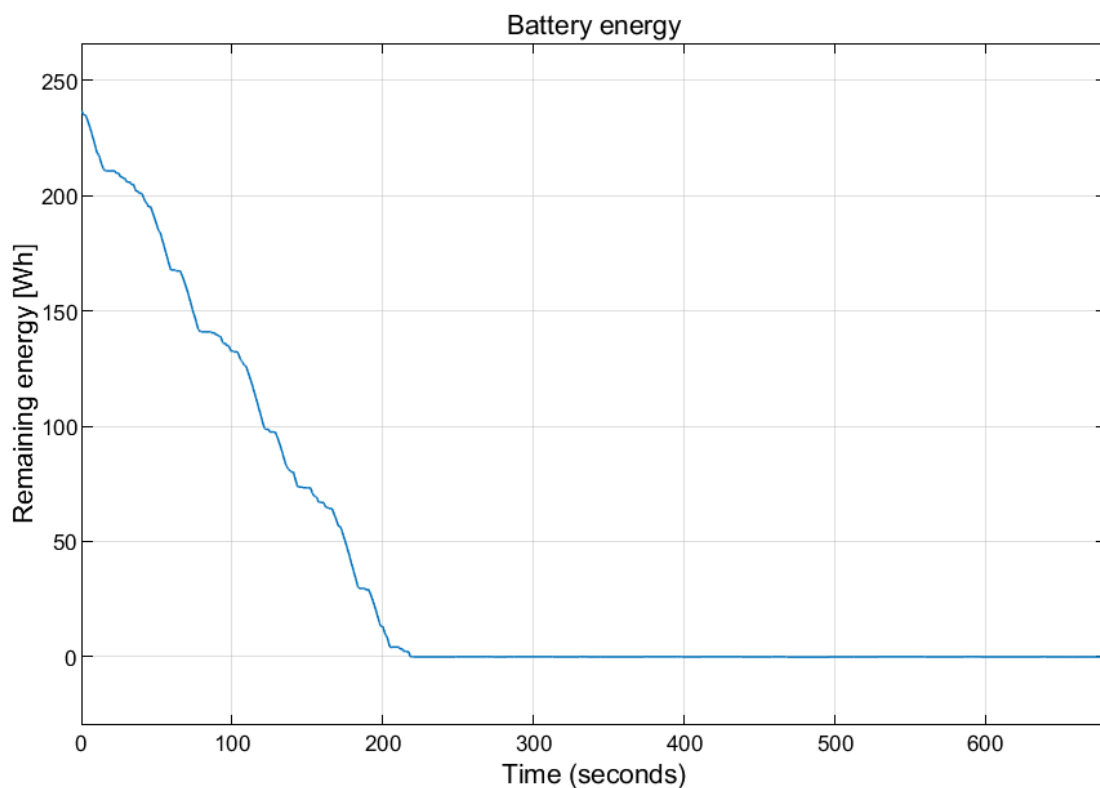


Figure 59 - energy usage on Endurance without energy saving and recuperation

The objective of the optimization is to tune parameters introduced in chapter 9 for the dynamic discipline Endurance. In all other disciplines the hybrid system can be utilized with maximum power without exhausting the battery.

With implementation of the recuperation control and energy saving from chapter 9, four parameters need to be tuned in the optimization task.

Table 9 - overview of optimization parameters

Parameter	Description
v_off	Speed, at which the front motors shut down to save energy (presumably at the end of straights).
v_recup	Speed at which the motors start generating (and braking) even under acceleration by the ICE
recup_acc	Value of braking torque applied to the motors after reaching speed v_recup .
recup_coast	Value of constant braking torque applied by the motors when the throttle pedal is not actuated

The objective function, Endurance time, then becomes a function of these four parameters.

$$t(v_{off}, recup_{acc}, recup_{coast}, v_{recup})$$

(10.1)

10.1. Genetic algorithms

Genetic algorithms borrow inspiration from biological evolution, where fitter individuals are more likely to pass on their genes to the next generation [29]. Fitness for reproduction of an individual in a randomly generated population is inversely related to the value of the objective function at that point. At each generation, the optimization parameters (genes) of the fitter individuals are passed to the next generation after undergoing the genetic operations of crossover and mutation. Genetic algorithms are global optimization algorithms and as such are suitable for this problem because of the unknown fitness landscape of our objective function.

To find the global minimum of our optimization problem, I first tried to use a genetic algorithm in Matlab's Global Optimization Toolbox. To examine the problem, first I optimized only the first half of Endurance to save computation

time. The optimization terminated after 62 generations and the results already improved the elapsed time substantially.

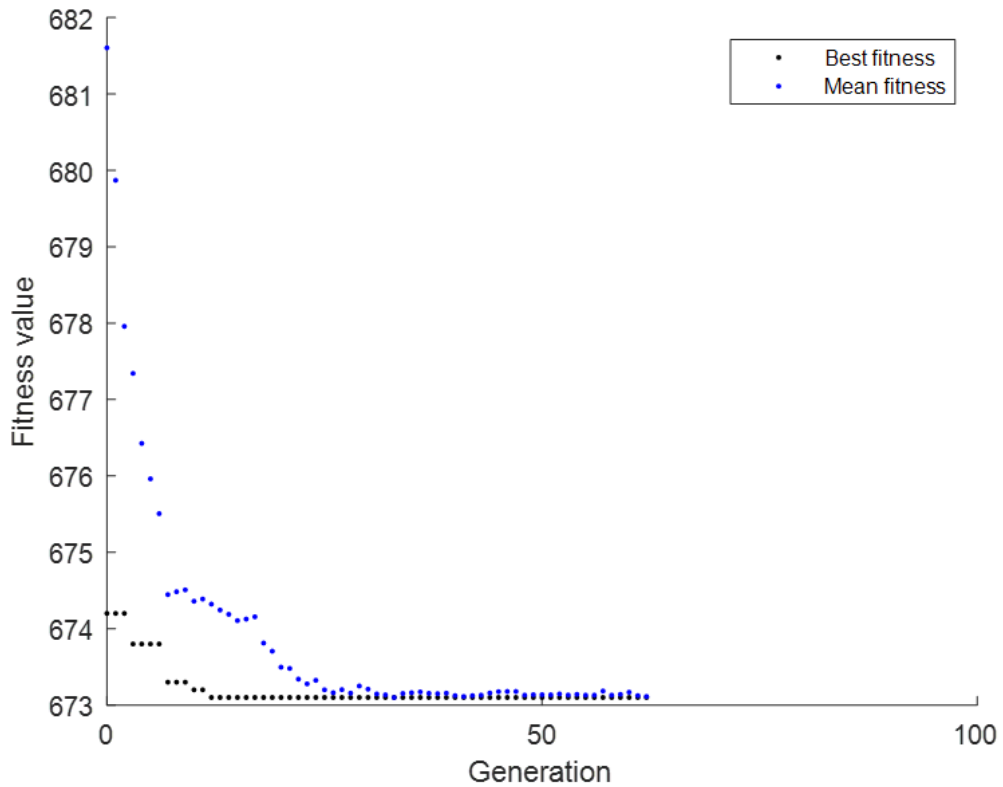


Figure 60 - optimization of first half of the Endurance using GA

The resulting time of the first half of the Endurance was 673.1 seconds and the parameters were the following:

Table 10 – resulting parameters after initial test of the optimization

Parameter	Value
v_off	18.5 m/s
v_recup	18.5 m/s
recup_acc	1.9 Nm
recup_coast	6.9 Nm
lap time	673.1 s

When examining the energy usage, we can see that implementing recuperation and energy saving allowed the system to spread the energy across the whole first half.

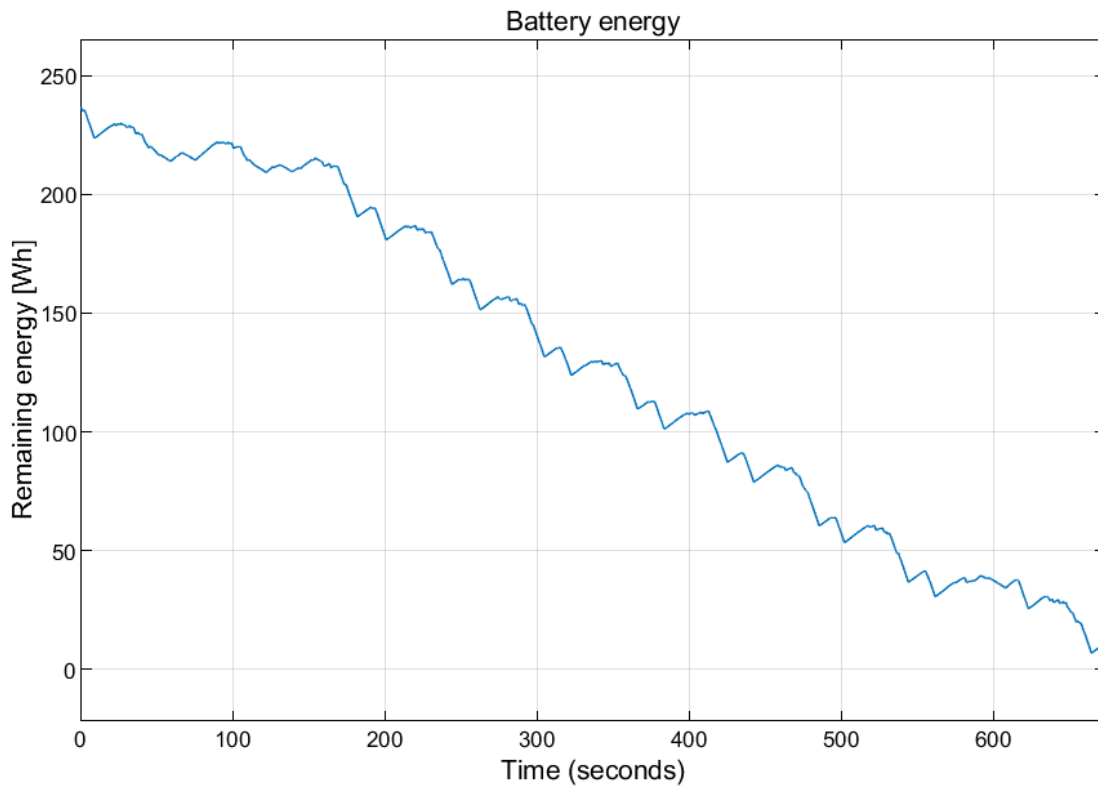


Figure 61 - energy usage on Endurance after optimization of the first half

To find the optimum over the whole distance of the Endurance, the resulting state of charge during the driver's change is plugged in as the starting state of charge of the second simulation. The optimization is then run again, but for each time result, the lap time simulation is run twice.

The next optimization terminates after 57 generations.

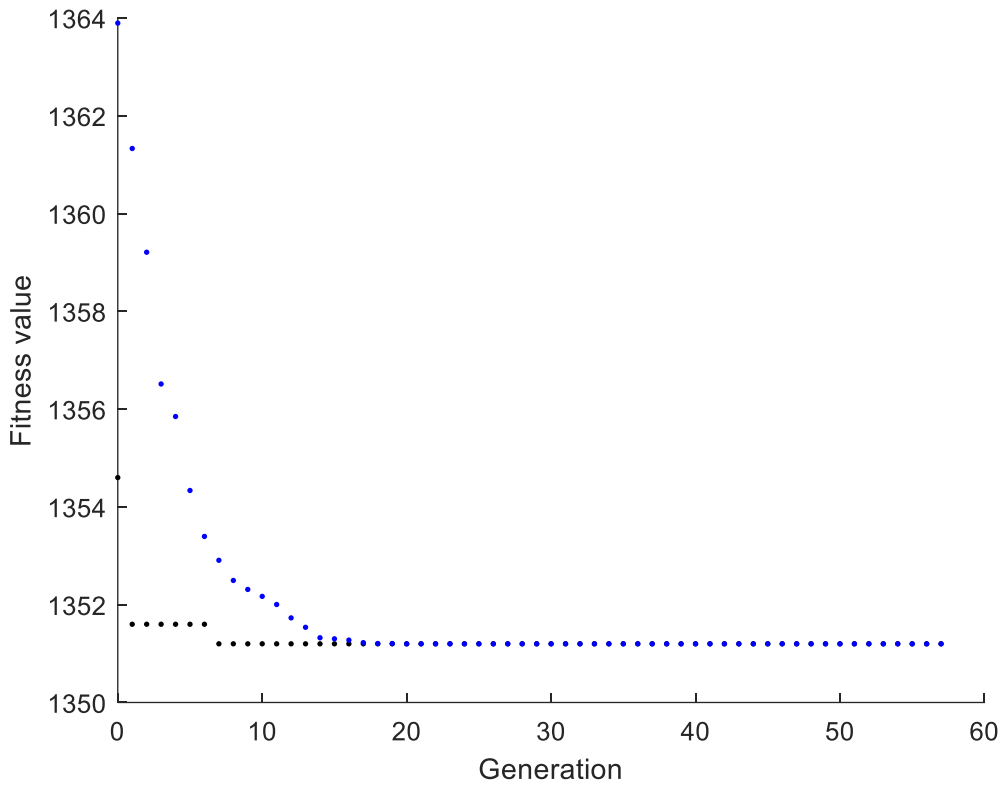


Figure 62 - optimization of the full Endurance using GA

The resulting time of the whole Endurance was 1351.2 seconds and the parameters were the following:

Table 11 - resulting parameters after full Endurance optimization using GA

Parameter	Value
v_off	17.1 m/s
v_recup	17.4 m/s
recup_acc	5.1 Nm
recup_coast	5.8 Nm
lap time	1351.2 s

From examination of the energy usage we can see, that both, the energy saving and recuperation are more aggressive, which allows the hybrid system to spread the energy usage across the whole distance of endurance.

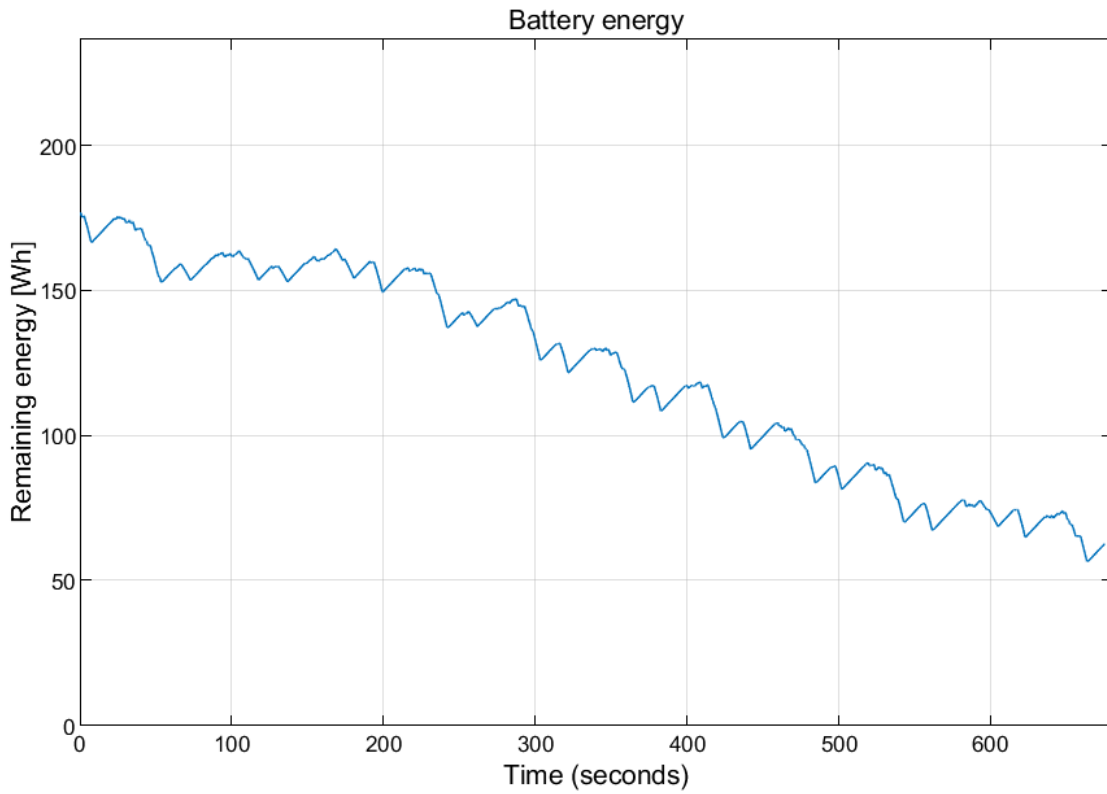


Figure 63 - energy usage on second half of Endurance after optimization over the whole distance using GA

From the energy usage in the second half we can also see, that the battery is not empty at the end of Endurance. This means there is unused potential and the optimum likely wasn't reached. To verify this claim, I tried to apply simplex optimization method.

10.2. Simplex method

For this optimization I used the `fminsearch` function in Matlab's Optimization Toolbox.

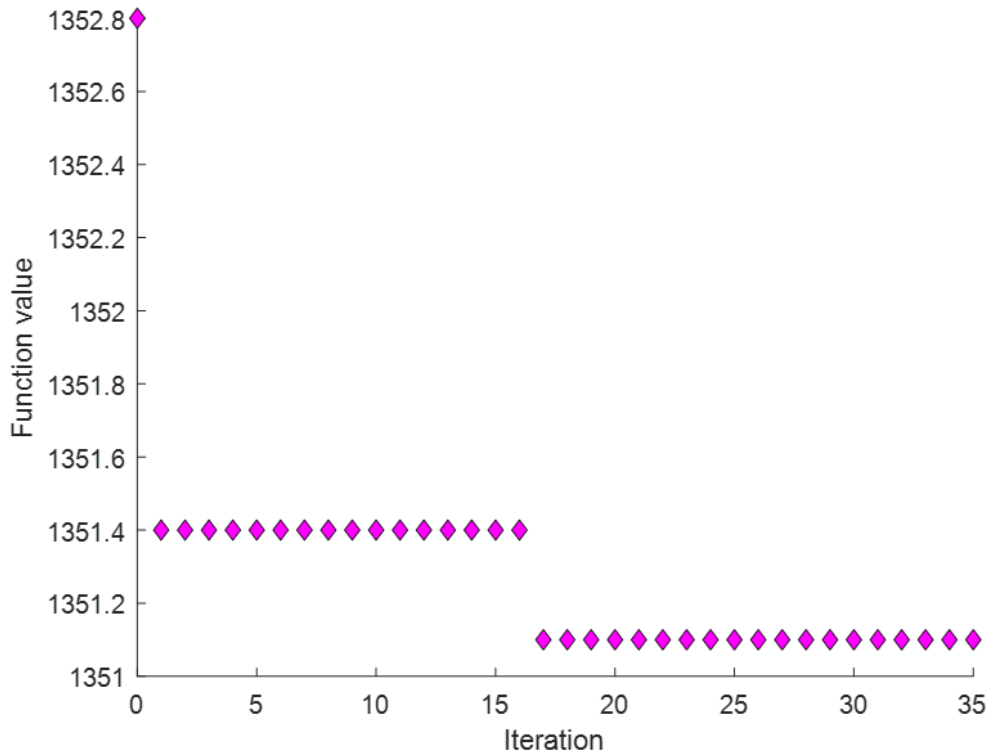


Figure 64 - optimization of the full Endurance using `fminsearch`

The results from this optimization show only a marginal gain in time.

Table 12 - resulting parameters after full Endurance optimization using `fminsearch`

Parameter	Value
v_off	17.1 m/s
v_recup	17.4 m/s
recup_acc	5.1 Nm
recup_coast	6.0 Nm
lap time	1351.1 s

Examination of the energy usage during the second half of the Endurance shows that the state of charge now got reasonably close to zero.

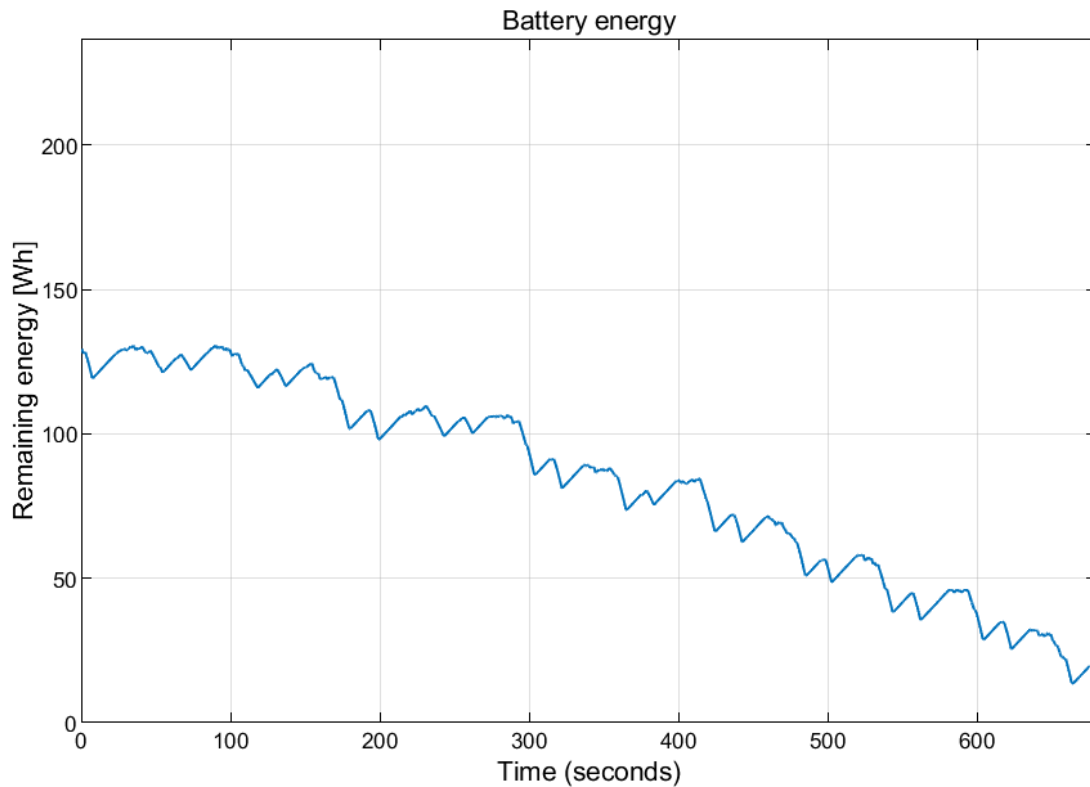


Figure 65 - energy usage on second half of Endurance after optimization over the whole distance using *fminsearch*

This result doesn't necessarily mean that the global optimum was reached, however, it shows that there is no obvious potential for further gain. The next step is to examine the sensitivity to change in the control parameters.

10.3. Sensitivity analysis

Any result from optimization, to be useful in the real world, must be reliably repeatable. That means that a small change in one of the parameters shouldn't significantly affect the value of the objective function. For this reason, I performed a simple sensitivity analysis by changing each of the parameters by 1% and observing the change in the resulting lap time.

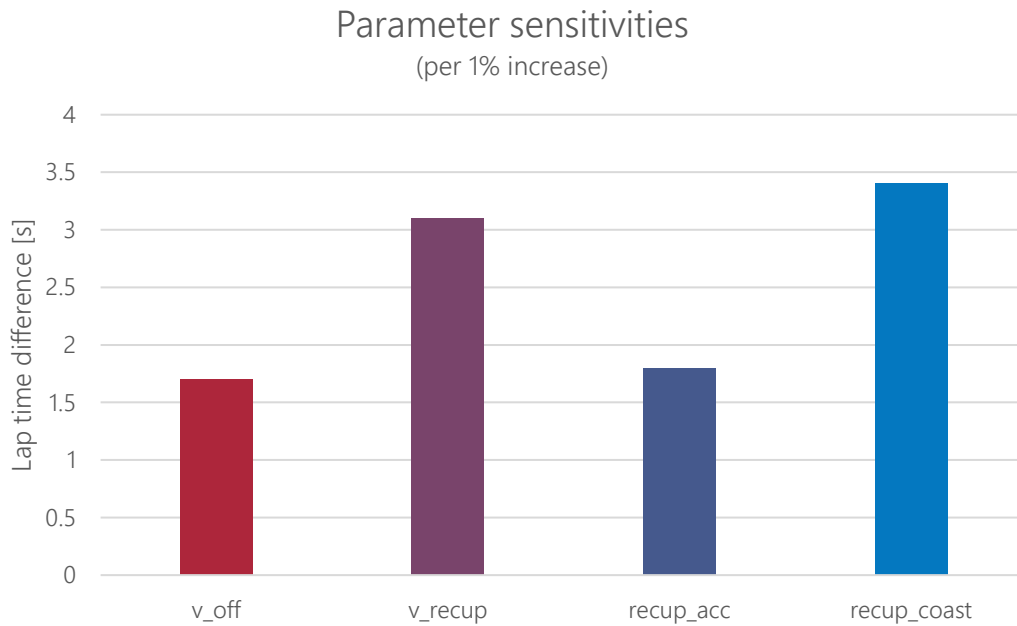


Figure 66 - results of sensitivity analysis

The results of the sensitivity analysis show, that even a small change to one of the parameters will affect the resulting time. The lap time is most sensitive to changes to recup_coast and v_recup parameters. Those can be affected by the motor controllers and the precise measurement of the vehicle speed. While 3.4 s change in the time of the whole endurance represents only an average change of 0.17 seconds per lap, a solution with less significant sensitivities might exist. In the next step of the optimization, I will optimize for two objective functions, namely the lap time and the sensitivity of the parameters.

10.4. Multi-objective optimization

Optimizing for multiple objective functions will result in a Pareto front. A Pareto front is a set of such results, that an improvement in one of the objective functions necessarily makes at least one of the others worse. Pareto fronts are useful when a tradeoff between two objectives must be made. In this case we are looking for a tradeoff between the parameter sensitivity and total lap time.

To calculate the Pareto front, a multi-objective genetic algorithm will be used. Namely the gamultiobj function in the Matlab's Global Optimization Toolbox.

One of the objective functions will be the same as in the previous optimizations:

$$t(v_{off}, recap_{acc}, recap_{coast}, v_{recup}) \tag{10.2}$$

The second objective function will be defined using the absmax Matlab function which takes a value from an array which has the maximal absolute value [30].

$$sensitivity = absmax(v_{off}^{sens}, recap_{acc}^{sens}, recap_{acc}^{sens}, v_{recup}^{sens}) \tag{10.3}$$

where the input values are the sensitivities of each of the control parameters used as inputs for the lap time simulation.

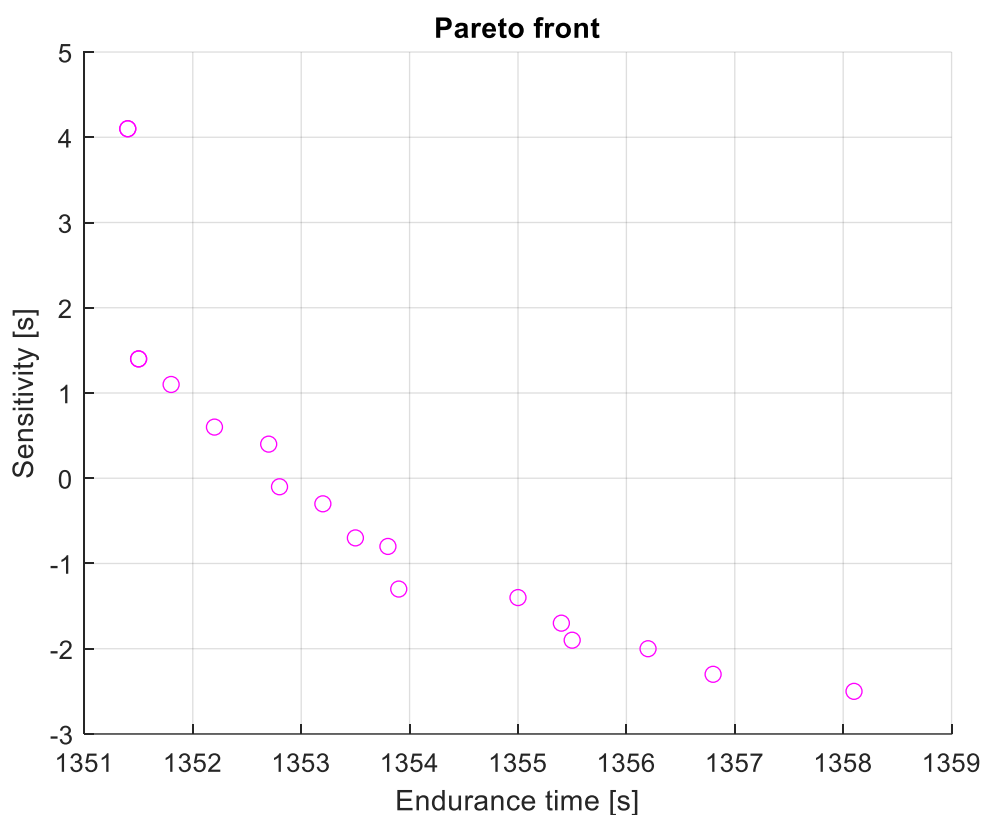


Figure 67 - Pareto front resulting from the multi-objective optimization

From the examination of the Pareto front we can see that the solutions approaching the 1351 second mark substantially increase in sensitivity. The solution with sensitivity closest to zero achieves a time of 1352.8 seconds, which is only 1.7 seconds slower than the best time. This seems as a good tradeoff and therefore, this point is chosen as the optimal control strategy.

10.5. Results

The results from optimization can be summarized in the following table.

Table 13 - overview of times per discipline after optimization

Discipline	FS.13 (no hybrid)	FS.14 (hybrid)	FS.14 (optimized hybrid)
Endurance	1352.8 s	1364.3 s	1352.8 s
Efficiency	3.03 l	3.00 l	2.98 l
Autocross	67.6 s	66.9 s	66.9 s
Skidpad	5.12 s	5.16 s	5.16 s
Acceleration	75	3.62 s	3.38 s

Implementation of the energy saving and recuperation strategy saves a total of 11.5 seconds on Endurance which roughly corresponds to 0.58 seconds per lap. Such time difference corresponds roughly to 10 points in Endurance scoring. The changes in fuel consumption are negligible.

11. CONCLUSION

All goals specified in the introduction of this thesis were achieved and the potential of an energy saving and recuperation algorithm for the FS.14 Formula Student monopost was thoroughly examined.

In chapter 3 I researched different hybrid vehicle concepts and approaches to optimization of energy consumption.

In chapter 6 I researched different methods of performing lap time simulations and compared their pros and cons which led me to a choice of a lap time simulation for this thesis.

In chapter 8 I adjusted the chosen lap time simulation and modified it by creating a model of the hybrid powertrain which allowed me to evaluate the benefit and the drawbacks of the additional electric motors and their battery to the overall performance of the vehicle.

In chapter 9 I designed a control algorithm for determining the driving and braking torques of the electric motors based on the driver's inputs with added features for energy saving and energy recuperation. Further, a concept of torque vectoring and traction control was proposed.

In chapter 10 an optimization of the proposed algorithm together with a sensitivity analysis of the proposed control parameters was performed. The sensitivity analysis provided an insight into the characteristics of the "fitness landscape" of the optimization and led to another objective function in order to minimize the sensitivity to the input parameters and thus make the system more robust. After creating a Pareto front consisting of the two objective functions an acceptable tradeoff between the achieved Endurance time and robustness (sensitivity) of the system was found.

Implementation of the algorithms and their optimization resulted in a time saving of 11.5 seconds on Endurance which corresponds to an expected gain of around 10 points in the discipline. Given that the implementation only requires a software update for the control unit of the hybrid system and doesn't have any obvious drawbacks (e.g. added weight), this is a substantial gain.

Full implementation of this algorithm in the real vehicle will require a thorough validation of the lap time simulation. A test track representative of an Endurance track must be constructed, then modelled in the simulation (using data from GPS) and the results from the simulation must be compared to the reality observed on the track. Firstly, the main parameters of the vehicle used in the simulation, such as the achieved longitudinal and lateral acceleration capabilities, the sensitivity to power, vehicle mass and aerodynamic effects must be validated with on-track measurements. This can be achieved by limiting the ICEs power in the engine control unit, using ballast weight and testing different aerodynamic setups. After that, the sensitivities of the new parameters of the control algorithm specific for the new test track should be compared to the sensitivities observed on the test track. A special effort should be given to the repeatability of such testing by measuring all external parameters that can further affect the vehicle performance, such as the weather conditions, track temperature, degradation of the tires and the consistency of the driver. Once the simulation is validated, a new optimization can be run either for each race track the vehicle will race on or on a whole set of tracks at once so that the parameters are universal for all tracks of a similar character. Such approach will likely yield worse overall results at the price of universality.

12. REFERENCES

- [1] Formula Student Germany, "FSG: Rules & Documents," 21 11 2021. [Online]. Available: https://www.formulastudent.de/fileadmin/user_upload/all/2022/rules/FS-Rules_2022_v1.0.pdf.
- [2] R. Garcia, J. Gregory and F. Freire, "Dynamic fleet-based life-cycle greenhouse gas assesment of the introduction of electric vehicles in the Portugese light-duty fleet," 2015.
- [3] A. Hajimiragha, C. A. Canizares, M. W. Fowler and A. Elkamel, "Optimal Transition to Plug-In Hybrid Electric Vehicles in Ontario, Canada, Considering the Electricity-Grid Limitations," vol. 57, no. 2, 2010.
- [4] M.-K. Tran, M. Akinsanya, S. Panchal, R. Fraser and M. Fowler, "Design of a Hybrid Electric Vehicle Powertrain for Performance Optimization Considering Various Powertrain Components and Configurations," vol. 3, no. 12, 2020.
- [5] S. Bhosle, K. Dedebyraktar, G. Buhariwala, M. Rahiman and A. Ahmed, "ENGINEERING A HYBRID SYSTEM," 2014.
- [6] [Online]. Available: <https://x-engineer.org/micro-mild-full-hybrid-electric-vehicle/>. [Accessed 3 8 2022].
- [7] [Online]. Available: <https://x-engineer.org/mild-hybrid-electric-vehicles-mhev-types/>. [Accessed 3 8 2022].
- [8] H. Seongmin, P. Taeho, N. Wonbin and L. Hyeongcheol, "Power distribution control algorithm for fuel economy optimization of 48V mild hybrid vehicle," Shanghai, 2017.
- [9] T. Boehme, B. Frank, M. Schultalbers, M. Schori and B. Lampe, "Solutions of Hybrid Energy-Optimal Control for Model-based Calibrations of HEV Powertrains," *SAE Technical Papers*, vol. 2, no. 4, 2013.

- [10] P. Denk, "Optimalizace jízdy silničního motorového vozidla," České vysoké učení technické v Praze, Fakulta strojní, Praha, 2019.
- [11] P. Polverino, I. Arsie and C. Pianese, "Optimal Energy Management for Hybrid Electric Vehicles Based on Dynamic Programming and Receding Horizon," *Energies*, vol. 14, no. 12, 2021.
- [12] S. Ebbesen, M. Salazar, P. Elbert, C. Bussi and C. H. Onder, "Time-optimal Control Strategies for a Hybrid Electric Race Car," *IEEE Transactions on Control Systems Technology*, vol. 26, no. 1, pp. 233-247, 2018.
- [13] R. Lot and S. Evangelou, "Lap Time Optimization of a Sports Series Hybrid Electric Vehicle," in *Proceedings of the World Congress on Engineering*, London, 2013.
- [14] M. Salazar, C. Bussi, F. P. Grande and C. H. Onder, "Optimal Control Policy Tuning and Implementation for a Hybrid Electric Race Car," *IFAC-PapersOnLine*, vol. 49, no. 11, pp. 147-152, 2016.
- [15] M. Salazar, C. Balerna, E. Chisari, C. Bussi and C. H. Onder, "Equivalent Lap Time Minimization Strategies for a Hybrid Electric Race Car," in *2018 IEEE Conference on Decision and Control (CDC)*, Miami, FL, USA, 2018.
- [16] Formula Student East, "Formula Student East," 19 9 2021. [Online]. Available: https://fseast.eu/wp-content/uploads/2022/01/FS_East_2022_Rules_v0.9.pdf.
- [17] W. F. Milliken and D. L. Milliken, *Race car vehicle dynamics*, SAE International, 1995.
- [18] C. Bachman, "Design Judges," 13 04 2022. [Online]. Available: <https://www.designjudges.com/articles/overall-vehicle-priorities>. [Accessed 15 08 2022].
- [19] T. Völkl, *Erweiterte quasistatische Simulation zur Bestimmung des Einflusses transienten Fahrzeugverhaltens auf die Rundenzeit von Rennfahrzeugen*, Audi Dissertationsreihe, 2013.
- [20] T. Novotný, "Lap Time Simulation," České vysoké učení technické v Praze, Praha, 2016.

- [21] CTU CarTech, internal documents of the team, *Engine dyno measurements*, 2019.
- [22] Y. Zhang, C. Zhao, B. Dai and Z. Li, "Dynamic Simulation of Permanent Magnet Synchronous Motor (PMSM) Electric Vehicle Based on Simulink," *Energies*, vol. 15, no. 3, 2022.
- [23] Plettenberg High End Elektromotoren-Manufaktur, *HP 620/40/A2 S P12 datasheet*, 2021.
- [24] LithiumWerks, "lithiumwerksbatteries.com," LithiumWerks, 3 2021. [Online]. Available: <https://store-cvt2jlgam8.mybigcommerce.com/content/LithiumWerks%20ANR26650M1-B%20Power%20Cell%20%28030921%29%20Data%20Sheet.pdf>. [Accessed 11 8 2022].
- [25] L. Martellucci and M. Giannini, "Regenerative Braking Experimental Tests and Results for Formula Student Car," vol. 11, no. 1, 2021.
- [26] E. D. Owen, *The Benefits of Four-Wheel Drive for a High-Performance FSAE Electric Racecar*, Massachusetts: Department of Mechanical Engineering, Massachusetts Institute of Technology, 2018.
- [27] F. Collin, "Traction Control for KTH Formula Student," KTH Royal Institute of Technology, School of Engineering Sciences, Stockholm, 2020.
- [28] J. A. Herring, K. J. Burnham and S. Oleksowicz, "Review and Simulation of Torque Vectoring Yaw Rate Control," 2012.
- [29] D. E. Goldberg, *Genetic Algorithms in search, Optimization, and Machine Learning*, Addison-Wesley, 1989.
- [30] A. McNeilly, "absmax," 2022. [Online]. Available: <https://www.mathworks.com/matlabcentral/fileexchange/41115-absmax>. [Accessed 13 8 2022].